



**Diogo Filipe  
Rocha Ferreira**

**PRIMING EVENTS AND DEVELOPMENT OF  
TOLERANCE UPON INFLUENZA A VIRUS AND  
*Staphylococcus aureus* INFECTION**

**EVENTOS DE PRIMING E DESENVOLVIMENTO DE  
TOLERÂNCIA APÓS INFEÇÃO COM O VÍRUS  
INFLUENZA A E *Staphylococcus aureus***

## DECLARAÇÃO

Declaro que este relatório é integralmente da minha autoria, estando devidamente referenciadas as fontes e obras consultadas, bem como identificadas de modo claro as citações dessas obras. Não contém, por isso, qualquer tipo de plágio quer de textos publicados, qualquer que seja o meio dessa publicação, incluindo meios eletrônicos, quer de trabalhos académicos.



**Diogo Filipe Rocha  
Ferreira**

**PRIMING EVENTS AND DEVELOPMENT OF  
TOLERANCE UPON INFLUENZA A VIRUS AND  
*Staphylococcus aureus* INFECTION**

**EVENTOS DE PRIMING E DESENVOLVIMENTO DE  
TOLERÂNCIA APÓS INFEÇÃO COM O VÍRUS  
INFLUENZA A E *Staphylococcus aureus***

Dissertação apresentada à Universidade de Aveiro para cumprimento dos requisitos necessários à obtenção do grau de Mestre em Microbiologia, realizada sob a orientação científica da Doutora Sónia Alexandre Leite Velho Mendo Barroso, Professora Auxiliar com Agregação do Departamento de Biologia da Universidade de Aveiro e coorientação da PD Doutora Christina Ehrhardt, Investigadora Principal no Instituto de Virologia de Münster.

Dedico este trabalho à minha família pelo apoio e pelas oportunidades que me proporcionaram.

## **o júri**

Presidente

Doutor Artur Jorge da Costa Peixoto Alves  
Investigador principal da Universidade de Aveiro

Doutora Cláudia Sofia Soares de Oliveira  
professora auxiliar convidada da Universidade de Aveiro

Prof. Doutora Sónia Alexandre Leite Velho Mendo Barroso  
professora auxiliar com agregação da Universidade de Aveiro

## **agradecimentos**

Quero agradecer, principalmente, e em primeiro lugar, à minha mãe, tios e primo e à restante família por todo o suporte durante toda a minha vida e, em particular, por todo o apoio dado durante este projeto. Por tudo, todos os momentos em que as forças falharam ou em que as saudades apertaram, todos juntos, conseguimos ultrapassar as dificuldades, e por isso, o meu obrigado.

Em segundo lugar, a todos os meus amigos, obrigado pelo apoio, pela ajuda, mas também por todos os bons momentos que partilhámos. Também quero agradecer a todos os professores e colegas que encontrei durante esta caminhada, por todas as adversidades que me ajudaram a ultrapassar e por todo o espírito de amizade e entreajuda que desenvolvemos juntos.

À Doutora Sónia Mendo, minha orientadora interna de mestrado, quero agradecer todo apoio prestado durante os dois anos de mestrado. Finalmente, quero agradecer à PD Doutora Christina Ehrhardt, minha orientadora externa, e ao Professor Doutor Stephan Ludwig, chefe do instituto, por me darem a oportunidade de desenvolver este projeto no Instituto de Virologia de Münster, por todo o aconselhamento e ajuda durante a adaptação a um país diferente, bem como por toda a assistência prestada durante a pesquisa científica e revisão do trabalho. À Doutora Christin Bruchhagen por toda a ajuda e por todas as horas passadas no laboratório. Ao Jens, à Gao, ao Felix, ao Andre e à Janine, bem como a todos os outros elementos do Instituto, agradeço por nos receberem tão bem e por todos os momentos e memórias que guardarei para sempre.

## **thankings**

I want to thank first and foremost my mother, uncles and cousin and the rest of the family for all the support throughout my life and in particular for all the support during this project. For all, the moments in which the forces failed or that the longings tightened, all together, we surpassed the difficulties, and, for that, my thanks.

Secondly, to my friends, for all support, help, but also for all the good times we share.

I would also like to thank all my colleagues and teachers, whom I encountered throughout this journey, for the difficulties that have helped me to cross and for all the spirit of friendship and mutual help we have developed together.

To Doctor Sónia Mendo, my master's internal advisor, I want to thank for all the support, during the two years of the master's degree.

Finally, I would like to thank PD Doctor Christina Ehrhardt, my external advisor, and Professor Stephan Ludwig, institute leader, for giving me the opportunity to develop this project at the Institute of Virology in Münster for guidance and help in adapting to a different country, as well, for all the assistance during the scientific research and work review. To Doctor Christin Bruchhagen, for all the help and hours spent in the lab.

To Jens, Gao, Felix, Andre, Janine and all the other elements of the Institute, for receiving us so well and for all the moments and memories that I will keep forever.

## palavras-chave

*Staphylococcus aureus*, influenza, coinfeção

## resumo

O vírus influenza é o agente causador da gripe, que se caracteriza como uma infecção respiratória aguda, de curta duração e é responsável por milhares de hospitalizações e mortes anuais, principalmente, devido a complicações que transformam infecções pelo vírus influenza em doenças mais graves, como infecções bacterianas secundárias. As infecções por *Staphylococcus aureus* (*S. aureus*) ocorrem durante, ou logo após a recuperação da infecção por influenza e estão associadas a maior morbidade e mortalidade. O resultado da doença é devido à resposta imune desregulada, associada ao aumento da expressão de citocinas e quimiocinas, aumento da carga de patogênicos e de lesões no tecido pulmonar. Este processo é regulado pela interação complexa e altamente dinâmica entre bactérias, vírus e o organismo hospedeiro. Embora alguns dos mecanismos causadores de infecções bacterianas secundárias sejam já conhecidos, o modo como uma exposição bacteriana primária afeta o desenvolver de uma infecção viral secundária ainda é limitado. Por essa razão, é importante entender os mecanismos subjacentes de como esse tipo de coinfeção se desenvolve. Modelos de infecção foram estabelecidos para reproduzir uma exposição bacteriana primária, seguida de uma infecção viral secundária, e assim, os resultados finais foram analisados. Para isso, várias técnicas, como Western-blotting e qRT-PCR, foram utilizadas de modo a avaliar a síntese proteica e de mRNAs, de elementos virais, bacterianos ou do hospedeiro, tais como, proteínas estruturais e ainda elementos de vias de sinalização. A morfologia celular foi outro parâmetro avaliado para determinar o sucesso e a extensão das infecções virais e, ou, bacterianas. Além disso, a quantificação da carga microbiana e viral foram também analisados. Estes mostram que, uma infecção bacteriana primária estimula as células hospedeiras para uma infecção secundária viral e que o desfecho desta, é pior do que em comparação com infecções com apenas cada um dos patogênicos. O dano é maior, as quantidades de agentes patogênicos aumentam, a resposta imune é maior e desregulada e mecanismos antivirais, como a resposta do IFN tipo I, são bloqueados, neste caso pela inibição da dimerização de STAT1-STAT2, pela bactéria. Concluindo, estes resultados mostram evidências de que uma infecção bacteriana estimula as células hospedeiras para uma infecção viral secundária.

**Keywords**

*Staphylococcus aureus*, influenza, coinfeção

**abstract**

Influenza viruses (IV) cause infections of the upper and lower respiratory tract and they are the causative agent of the flu, which causes several thousand hospitalizations and deaths each year, due complications that turn IV infections into more serious diseases, like secondary bacterial infections. *Staphylococcus aureus* (*S. aureus*) infections occur during and/or shortly after recovery from influenza and they are associated with increased morbidity and mortality. The disease outcome is due to deregulated immune response associated with increased cytokine and chemokine expression, enhanced pathogen load and tissue lesions. This process is regulated by complex and highly dynamic interaction between bacteria, virus, and the host organism. Although some of the mechanisms leading to secondary bacterial infections are known, the knowledge on how primary bacterial exposure will affect the course of a secondary viral infection is still limited. For this reason, it is important to understand the underlying mechanisms of how this type of co-infections develop. Then, infections models were established in order to mimic a primary bacterial exposure, followed by a secondary viral infection and the outcomes were analyzed. For that, techniques like Western-blotting and qRT-PCR, were performed in order to determine the protein and mRNA synthesis of viral, bacterial and host structural and signaling pathways protein elements. Cell morphology was also evaluated to determine the success and extention of viral and or bacterial infections. Besides that, pathogen loads were also quantified and analyzed. Results show that, a primary bacterial infection primes the host cells towards post viral infection and that the outcome is worse than compared to single infections. Tissue damage is higher, pathogen loads increase, immune response is exacerbated and anti-viral mechanisms, like the type I IFN response is blocked, by inhibition of STAT1-STAT2 dimerization. With this, there is evidence that a bacterial infection, primes the host cells for a secondary viral infection.

## Index

1. Introduction.....	4
1.1. Influenza virus.....	4
1.1.1. IAV morphology and genome.....	6
1.1.2. Life cycle.....	7
1.2. Immune response upon IAV infection.....	8
1.3. <i>Staphylococcus aureus</i> .....	11
1.3.1. <i>S. aureus</i> infection.....	12
1.4. Immune response upon <i>S.aureus</i> .....	13
1.5. IAV and <i>S. aureus</i> infection.....	15
1.6. Pathogenesis of co-infection.....	16
1.7. Influence of prior bacterial exposure upon viral infection.....	17
1.8. Study aims.....	18
2. Material.....	20
2.1. Equipment and material.....	20
2.2. Software.....	22
2.3. Chemicals and reagents.....	22
2.4. Nutrients and additives.....	24
2.5. Material for cell culture.....	25
2.6. Medium and buffers.....	25
2.7. Kits.....	28
2.8. Primer.....	29
2.8.1. Primers for qRT-PCR.....	29
2.8.2. Other Oligonucleotides.....	30
2.9. Antibodies.....	31
2.9.1. Primary Antibodies.....	31
2.9.2. Secondary Antibodies.....	31
2.10. Cell lines.....	32
2.11. Pathogens.....	32
2.11.1. Virus.....	32
2.11.2. Bacteria.....	32
3. Methods.....	33

3.1. Cell culture.....	33
3.2. Virological methods.....	33
3.2.1. Virus propagation.....	33
3.2.2. Determination of infectious virus titres (standard plaque assay).....	34
3.3. Bacteriological methods.....	34
3.3.1. Cultivation.....	35
3.3.2. Determination of colony-forming bacterial titers.....	35
3.4. Co-infection model.....	36
3.4.1. Infection with <i>S. aureus</i> and IAV.....	36
3.5. Molecular biological methods.....	37
3.5.1. Nucleic acids.....	37
3.5.1.1. RNA extraction.....	37
3.5.1.2. Determination of nucleic acid concentrations.....	38
3.5.1.3. Reverse transcription.....	38
3.5.1.4. Quantitative real-time PCR.....	38
3.5.2. Proteins.....	39
3.5.2.1. Preparation of protein lysates.....	39
3.5.2.2. Determination of protein concentrations.....	40
3.5.2.3. Discontinuous SDS polyacrylamide gel electrophoresis (SDS-PAGE) .....	40
3.5.2.4. Western Blot and immunodetection.....	41
3.5.2.5. Determination of cytotoxicity by activity measurement of Lactate dehydrogenase (LDH).....	42
3.5.2.6. Detection of secreted cytokines and chemokines via Fluorescence- activated cell sorting (FACS).....	42
4. Results.....	44
4.1. Bacterial and viral co-infection increases the cell damage and death.....	44
4.2. Pathogen load is enhanced upon co-infection.....	46
4.3. Immune response.....	50
4.3.1. Induction of type I IFN- $\beta$ and downstream factors is enhanced in presence of IAV and <i>S. aureus</i> .....	51
4.3.2. Phosphorylation of STAT1 and mRNA synthesis of downstream elements are reduced upon co-infection.....	53
4.3.3. Cytokine and chemokine expression are increased during co-infection .....	56

4.3.4. IL-18 secretion is increased during co-infection.....	57
5. Discussion.....	59
5.1. Cell damage is increased upon co-infection.....	59
5.2. Cytokine and chemokine are enhanced during viral and bacterial co-infection.....	60
5.3. Blockade of anti-viral response.....	61
6. Conclusion.....	63
7. References.....	64

## Figure Index

Figure 1 – An influenza A virus virion.....	7
Figure 2 – IFN-induced JAK-STAT signaling pathways.....	10
Figure 3 – <i>Staphylococcus aureus</i> cell structure and pathogenic factors.....	13
Figure 4 – Inflammasome activation leading to production of IL-18 and IL-1 $\beta$ cytokines.....	15
Figure 5 - 32 and 48 hours infection scheme of a secondary viral infection after primary <i>S. aureus</i> infection.....	36
Figure 6 - Cell damage is increased in co-infected cells.....	45
Figure 7 - Viral and bacterial titers are enhanced upon co-infection.....	47
Figure 8 - Upon co-infection mRNA and protein synthesis of both pathogens is increased. A549 cells were incubated with <i>S. aureus</i> 6850 wt (MOI 0.001) for 3 h.....	49
Figure 9 - Expression of type IFN- $\beta$ and ISGs is enhanced upon viral and bacterial co-infection.....	52
Figure 10 - Phosphorylation of STAT1 and mRNA synthesis of downstream factors are reduced upon co-infection.....	54
Figure 11 - Cytokine and chemokine expression is increased upon co-infection...	56
Figure 12 - The IL-18 protein synthesis and secretion is increased upon co-infection.....	58

## Introduction

Influenza viruses (IV) cause infections of the upper and lower respiratory tract and they are the causative agent of the flu, which causes several thousand hospitalizations and deaths each year. Severe illness evolves in very young or old and immunosuppressed patients and there are several ways to develop IV infections into more serious diseases, like secondary bacterial infections. *Staphylococcus aureus* (*S. aureus*) infections occur during and/or shortly after recovery from influenza and they are associated with increased morbidity and mortality. They can also occur in young and immunocompetent patients and the disease outcome is due to deregulated immune response associated with increased cytokine and chemokine expression, enhanced pathogen load and tissue lesions. This process is regulated by complex and highly dynamic interaction between bacteria, virus, and the host organism. These interactions will lead to changes in the host or even in the pathogens, since they will modulate the environment to take benefit from it. Although some of the mechanisms leading to secondary bacterial infections are known, the knowledge on how primary bacterial exposure will affect the course of a secondary viral infection is still limited. For this reason, it is important to understand the underlying mechanisms of how this type of co-infections develop, to estimate pathogenicity and to create new therapies to fight this kind of disease, since for example the emergence of bacterial resistant strains is a major concern in modern medicine.

### 1.1. Influenza virus

IV are the causative agents of the disease commonly known as the flu, which is associated with mild symptoms, but also high fever, coryza, cough, headache, prostration, and fatigue (Taubenberger and Morens, 2008).

IV, together with Isa- and Thogoto virus, belong to the *Orthomyxoviridae* family that clusters enveloped viruses with negative-sense single-stranded RNA (ssRNA) segmented genomes (Taubenberger and Kash, 2010). IV can be subdivided into 4 genera, influenza A (IAV), B (IBV), C (ICV) and the recently described influenza D (IDV) viruses (Hause et al., 2014). Their distinction is

based on serological characteristics of their nucleoproteins (NP) and matrix proteins (M1 and M2) (Lamb, Krug and Knipe, 2001), which are major structural components of their virions (Noda, 2012). IAV are also subdivided by antigenic characterization of haemagglutinin (HA) and neuraminidase (NA) surface glycoproteins of the virion (Tong *et al.*, 2013, Bouvier and Palese, 2008). IAV and IBV genomes have eight genomic segments, while ICV and IDV only have 7 segments (Cheung and Poon, 2007, Nakatsu *et al.*, 2018). Influenza A, B, C and D also differ in their host range and pathogenicity (Taubenberger and Morens, 2008, Nakatsu *et al.*, 2018). IDV was recently isolated from swine and cattle (Nakatsu *et al.*, 2018). Although, ICV can be isolated from pigs and dogs and IBV from seals (Brown, 1995, Osterhaus, 2001), the influenza B and C types are almost exclusively isolated from humans, whilst IAV have a broader host spectrum, infecting birds, humans, horses, swine, and other mammals (Taubenberger and Morens 2008). Aquatic birds are the natural reservoir for all the IAV and the potential source of the human pandemic influenza strains (Webster, 1992).

IAV and IBV are responsible for illness in humans and seasonal epidemics that result in several thousand deaths per season worldwide (Iuliano *et al.*, 2017). In the case of IAV, epidemics are caused by the lack of proofreading function of the viral RNA-dependent RNA polymerase, which creates antigenic drift variants and due to changes in the HA and NA epidemics occur (Fodor and Velthuis, 2016). However, IAV are also relevant in human pathogenicity, since they have the potential to develop pandemic virus variants (Taubenberger *et al.*, 2010). The most prominent example of these pandemics is the Spanish flu of 1918-1919, which caused more than 50 million deaths (Johnson and Mueller, 2002). As said before IAV has a segmented genome, which allows the exchange of viral genome segments between different strains, which is known as antigenic shift. Thus, upon host infection with more than one IAV strain, generation of reassortant viruses is possible, generating new strains with novel characteristics that might be able to cause pandemics (Scholtissek, 1995, Nelson and Holmes, 2007, Bouvier and Palese, 2008).

### **1.1.1. IAV morphology and genome**

IAV are enveloped particles surrounded by a lipid bilayer originated from the host cell that contains lipid rafts (Scheifelle *et al.*, 1999). The particles are pleomorphic, they can be spherical or filamentous (Dadonaite, 2016; Chu *et al.*, 1949) and range from 80 to 120 nm in diameter (Elford *et al.*, 1936). However, filamentous structures can reach lengths of several micrometers. The genetic background and the method of virus culture influence the morphology of the virus particles (Roberts, 1998). The eight segments that form the viral genome encode for at least 10 viral genes: HA, NA, matrix 1 (M1), matrix 2 (M2), nucleoprotein (NP), non-structural protein 1 and 2 (NS-1 and NS-2, which is known as nuclear export protein, NEP), polymerase acidic protein (PA) and polymerase basic proteins 1 and 2 (PB1 and PB2) (Klemm *et al.*, 2018). The viral envelope, derived from the host membrane, is formed by a lipid bilayer that contains three viral transmembrane proteins: HA, NA and M2. M1 is located below this bilayer forming a matrix that surrounds the viral ribonucleoproteins (vRNPs), which are made of viral negative stranded RNAs wrapped around NP and small amounts of NEP. At the end of the vRNPs there are three polymerase proteins (PB1, PB2 and PA) that form the viral RNA polymerase complex (Samji, 2009; Nayak, 2004; Nayak, 2009).

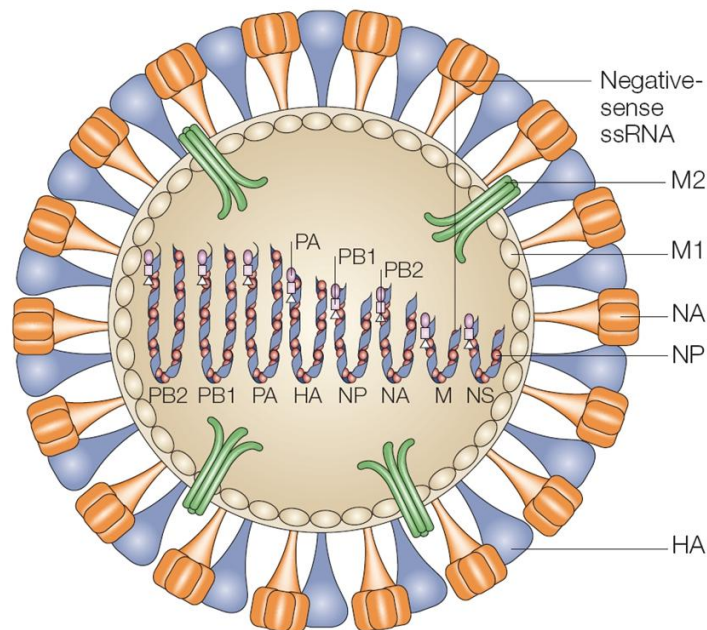


**Figure 1 – An influenza A virus virion.** Two surface glycoproteins, hemmagglutinin (HA) and neuraminidase (NA), and M2 ion-channel are embedded in the viral envelope, which is derived from host's cellular membrane. The RNP complex is composed by a viral RNA segment associated with the nucleoprotein (NP) and three polymerase proteins (PB1, PB2 and PA). The matrix (M1) protein associates with the RNP and the viral envelope (Horimoto, T. *et al.*, 2005)

### 1.1.2. Life cycle

During infection, influenza virions attach to the host respiratory tract epithelial cells, by the binding of viral HA to the sialic acids on the host cell (Morris, 2017). There are two major linkages between sialic acids and the carbohydrates they are bound to in glycoproteins that determine species specificity:  $\alpha(2,3)$  and  $\alpha(2,6)$ . Human virus recognize the  $\alpha(2,6)$  link, while avian recognize  $\alpha(2,3)$  linkages. Swine viruses recognize both (Skehel, 2000). After binding to the host cell's sialic acid residues, virions are internalized into the endosome by receptor-mediated endocytosis. The endosome has a low pH, between 5 and 6, which triggers the fusion of the endosomal and viral membranes, mediated by a conformational change in HA (Skehel, 2000; Huang *et al.*, 2003). The acidic

environment also opens the M2 ion channel (Pinto, 1992), resulting in an acidification of the viral core, which causes the dissociation of the vRNP from M1 (Pinto, 2006). These two events provoke the release of the vRNPs to the cell cytoplasm.

After being internalized the viruses use the cell machinery to replicate, transcribe viral RNA and to produce viral components. For this to happen, after being released into the cytoplasm, the vRNPs must enter the nucleus. The import occurs via the Crm1 dependent pathway, by vRNP binding to proteins involved in the nuclear import, like for example importin  $\alpha$  and  $\beta$  (Görlich *et al.*, 1994).

Replication does not require a primer, since the viral RNA dependent polymerase (RdRp) is responsible for the primer-independent initiation of replication. Genome transcription only occurs after conversion into complementary positive sense RNA (cRNA), which will serve as a template to produce new viral RNAs. Since the IAV genome has a small size (13-16 kb), IAV use the host cell's machinery for its own purpose. PB2, one of the RdRp proteins, has endonuclease activity and binds to the 5' methylated caps of cellular messenger RNA (mRNA) and cleaves it (Velthuis, 2014; Fodor, 2013; York and Fodor, 2013). The cellular capped RNA fragment is used by the viral RdRp as a primer for viral transcription (Li, Rao, and Krug, 2001). This mechanism is called cap-snatching (Krug *et al.*, 1979; Dhar, 1980). Then the export of the vRNPs from the nucleus is done via the CRM1 dependent pathway through nuclear pores (Boulo *et al.*, 2007). After vRNP release out of the nucleus, viral particles are built and progeny viruses bud from the cell, surrounded by the host cell membrane. The new viral particle can then leave the membrane after the cleavage of the sialic acid residue by the NA (Palese *et al.*, 1974). Once it is free, the viral progeny will spread the infection throughout the neighboring cells.

## **1.2. Immune response upon IAV infection**

IAV infect airway and alveolar epithelial cells, and as explained, they are dependent on the host cells for their replication. This means that IAV use the

cellular functions to their advantage, but concomitantly they must bypass the cellular defense mechanisms. The innate immune response is the first line of defense against viral infection, characterized by rapid but nonspecific responses. As the infection progresses, the virus causes cell damage and death in the host airways. Particularly, the production of virulence factors, like PB1-F2 and NS1 is enhanced that cause even further destruction such necrosis of the host cells (Conenello *et al.*, 2007; Iverson *et al.*, 2011). Pandemic influenza infections are also known for generating increased inflammation response due to excessive expression of cytokines and chemokines (Rock and Kono, 2008).

During IAV infection, viral conserved components called pathogen associated molecular patterns (PAMPs) are recognized by host pathogen recognition receptors (PRRs), such as: retinoic acid-inducible gene-I protein (RIG-I) and toll-like receptor (TLR). PRRs induce the activation of innate immune signaling and the production of various cytokines and antiviral molecules (Ouyang, 2014). RIG-I is the main receptor, which recognizes intracellular ssRNA and other transcribed intermediate products of IAVs in infected host cells. After recognition of PAMPs, RIG-I gets activated and stimulates MAVS. The downstream transduction signaling at the outer mitochondrial membrane takes place and (Yoneyama, 2015) activates interferon regulatory factor 3 (IRF3), IRF7 and nuclear factor kappa-light-chain-enhancer of activated B cells (NF- $\kappa$ B). This results in the expression of interferons (IFNs) and pro-inflammatory cytokines (Hiscott, 2006). While TLR1, 2, 4, 5 and 6 are expressed on the cell membrane and recognize PAMPs derived from bacteria, fungi, and protozoa, TLR3, 7, 8 and 9 are expressed of endosome and lysosome surfaces and recognize nucleic acid PAMPs derived from viruses, including IAV (Kumar, 2011). In endosomes TLR3 recognizes dsRNA (Alexopoulou *et al.*, 2001) and TLR7 recognizes ssRNA of influenza virions (Lund, 2004). Also, some NOD-like receptors (NLRs), like NLR family pyrin domain containing 3 (NLRP3) are activated upon cellular infection with IAV (Philpott, 2014), inducing pro-inflammatory cytokines (Gross, 2011).

Type I IFNs, such as IFN- $\alpha$  and IFN- $\beta$ , and type III IFNs, known as interferon lambdas (IFN- $\lambda$ ) 1, 2, 3, 4 and 5 play important roles in virus infected cells (Levy *et al.*, 2011). IAV infection induces strong expression of type I and III IFN genes (Wang, 2009). IFN- $\alpha$  and IFN- $\beta$  interact with IFN- $\alpha$ /IFN- $\beta$  receptors (IFNAR), activating Janus kinase-signal transducer and activator of transcription (JAK-STAT) signaling pathway (Ehrhardt, 2010). Phosphorylated STAT1 (pSTAT1) and STAT2 bind to IRF9 to form the IFN-stimulated gene factor 3 (ISGF3), which translocate into the nucleus and attaches to IFN-stimulated response element (ISRE), leading to transcription of several IFN-stimulated genes (ISGs) (Ehrhardt, 2010; Garcia-Sastre, 2011). ISGs act on different steps of IAV life cycle. Some restrict viral entry into the cells, like the Mx family (Chen, 2018). Mx family gathers human myxovirus resistance protein A and B (MxA and MxB) in humans, and they are produced by various cells, such as hepatocytes, endothelial cells, and immune cells (Fernández and Quiroga, 1999). Others, like ISG15, restrict viral replication by interfering with virus release and translation of viral proteins (Yuan, 2001).

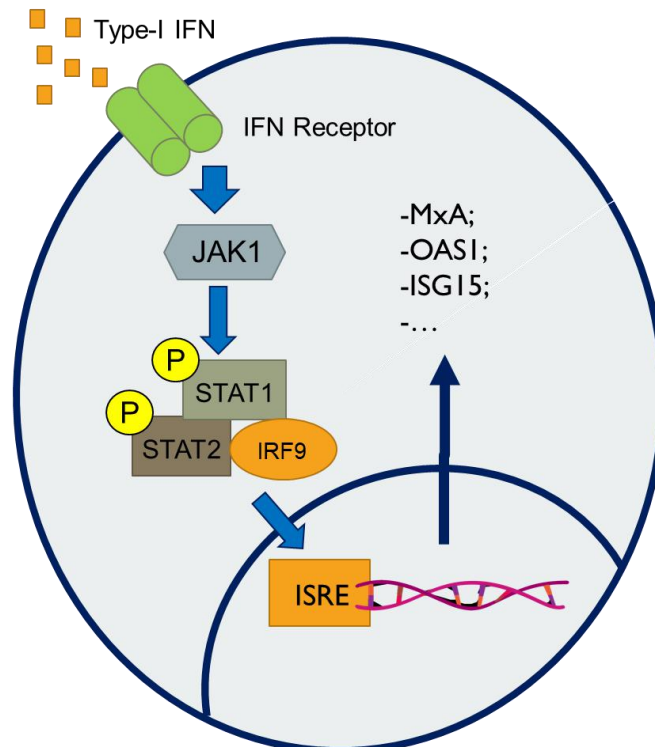


**Figure 2 – IFN-induced JAK-STAT signaling pathways.**

This protein also promotes enhanced expression of pro-inflammatory cytokines, through activation of NF- $\kappa$ B (Reis and McCauley 2013). The translocation of PB1-F2 to the mitochondria provokes the loss of membrane potential and fragmentation of the organelle, as explained before and also provides signals for activation of pro-inflammatory cytokines (Pinar, 2017).

### **1.3. *Staphylococcus aureus***

*S. aureus* is a member of the *Staphylococcaceae* family and it is a globular gram-positive bacterium that forms clusters. It is also distinguishable from other staphylococcal species by its gold pigmentation of colonies and positive results of coagulase, mannitol-fermentation and deoxyribonuclease tests. (Lowy, 1998). The main component of the *S. aureus* cell wall is peptidoglycan (PGN), which consists of alternating polysaccharide subunits of *N*-acetylglucosamine and *N*-acetylmuramic acid with 1,4- $\beta$  linkages. Ribitol teichoic acids and lipoteichoic acids (LTA) are also found in the bacterial cell wall. Its genome consists of a circular chromosome as well as extrachromosomal genetic elements, such as prophages, plasmids, and transposons (Lowy, 1998).

It is both a commensal bacterium and a human pathogen and colonizes approximately 30% of the human population (Kluytmans *et al.*, 1997). People with type 1 diabetes, surgical patients, patients undergoing hemodialysis or with acquired immunodeficiency syndrome, but also intravenous drug users, have high rates of *S. aureus* colonization accompanied by an increasing risk of a subsequent infection (Lowy, 1998). *S. aureus* is a leading cause of bacteremia as well as osteoarticular, skin, soft-tissue and pleuropulmonary infections (Tong *et al.*, 2015) and in some cases, these infections are reported to persist asymptotically with relapses occurring months or even years after anti-microbial therapy (Cabot *et al.*, 1993; Kipp *et al.*, 2003, Proctor *et al.*, 1995).

It develops in very young and old group ages and represents a major human pathogen (Tabah *et al.*, 2012). Furthermore, the worldwide increase of

infections caused by methicillin resistant *S. aureus* strains (MRSA) is a major cause for concern (Wertheim *et al.*, 2005).

### **1.3.1. *S. aureus* infection**

*S. aureus* has a diverse arsenal of components and products that contribute to the pathogenesis of infection, as toxins, like the protein-alpha toxin, that causes pore formation and induces pro-inflammatory changes in mammalian cell walls, adhesins, enzymes or other components like proteases, lipases that destroy tissue and facilitate the spread of the infection (Gordon and Lowy, 2008). Another example is the Panton-Valentine Leucocidin (PVL), which is a cytotoxin that causes leukocyte destruction and tissue necrosis (Lina *et al.*, 1999). Resistance related factors, such as the  $\beta$ -Lactamase enzyme that confers resistance against  $\beta$ -lactam antibiotics, are also important for the maintenance and persistence of infection (Fuda *et al.*, 2005).

These entire mechanisms of bacterial pathogenicity make *S. aureus* infections difficult to treat. Thus, *S. aureus* infections still represent serious and costly clinical problems (Tuchscherer *et al.*, 2011).

Infections are initiated when a physical breach of the skin of the mucosa allow the bacteria to access the tissue or the bloodstream, and the acute phase of the disease is determined by the expression of multiple bacterial virulence factors, which enable *S. aureus* to adhere to host structures, destroy tissue, and invade host cells (Tuchscherer, 2010). In some cases, these infections are reported to persist asymptomatically with relapses occurring months or even years after anti-microbial therapy (Cabot, 1993; Kipp *et al.*, 2003, Proctor *et al.*, 1995). Intracellular bacterial persistence is a mechanism used by the bacteria to bypass the antibacterial immune response that leads to the formation of chronic infections (Lowy, 2008; Tuchscherer, 2010), which have been largely associated with altered bacterial phenotype, like small-colony variants (Proctor, 2006).

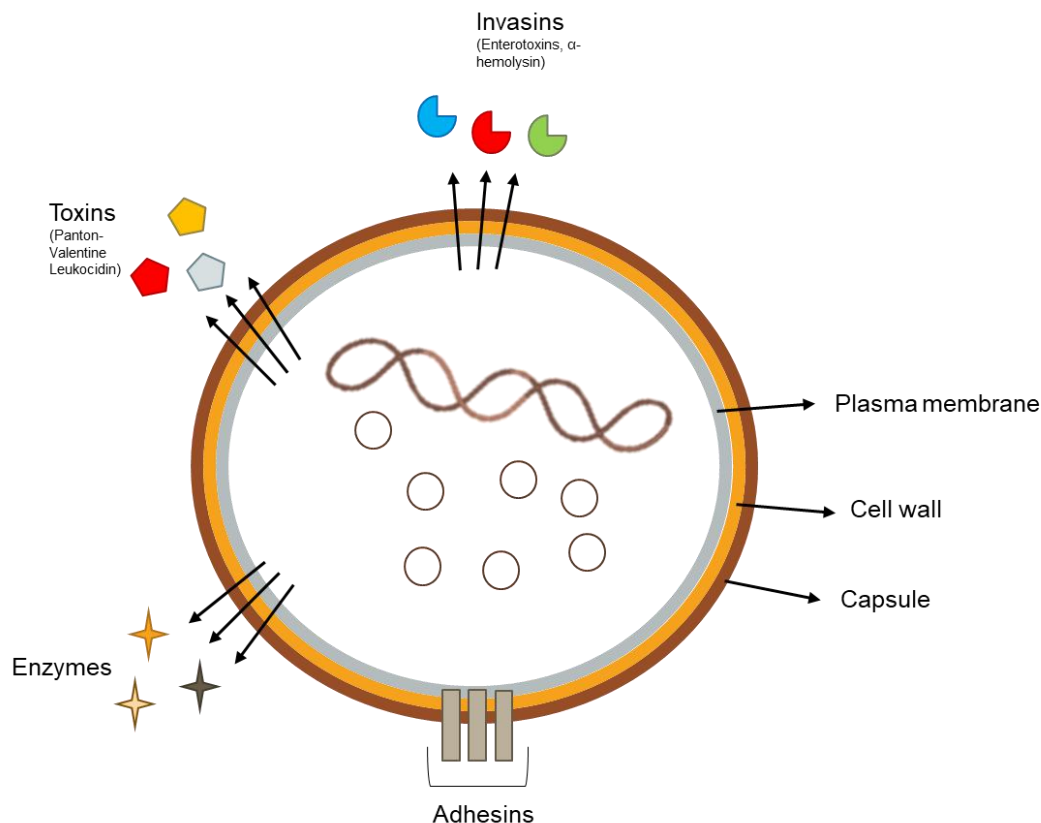


**Figure 3 – *Staphylococcus aureus* cell structure and pathogenic factors.** *S. aureus* has a complex cell wall structure composed of a thick peptidoglycan layer and polysaccharide capsule. Besides that, it also possesses an arsenal of structural and secreted virulence factors involved in cytotoxicity, adherence and invasion of host tissue and immune invasion.

#### 1.4. Immune response upon *S.aureus*

Bacterial factors that allow *S. aureus* to switch from a commensal bacterium to an invasive infection status are still unknown, although, the intensity of the immune response caused by the bacterium, seems to have a prominent role in the infection severity.

Airway epithelial cells are responsible for the initial immune signaling, recruiting immune cells, including dendritic cells, macrophages, and T cells. The result of this immune signaling is the recruitment of polymorphonuclear neutrophils (PMNs) (Parker and Prince, 2012)

This response is started upon the recognition of *S. aureus* components by PRRs localized on the surface of airway epithelial cells. These cells express

all the TLRs, as well as RNA receptors, like MDA5 and RIG-I (Gómez *et al.*, 2004; Xing and Harper *et al.*, 2011). TLR2 has an important role on *S. aureus* infection, since it recognizes LTA of the bacterial cell wall. The LTA presence results in significant inflammation and neutrophil recruitment (von Aulock, 2003; Hoogerwerf *et al.*, 2008). Via TLR2-mediated signaling the PVL directly activates a set of genes that lead to NF- $\kappa$ B induction (Zivkovic *et al.*, 2011). The *S. aureus* infection through the TLRs causes the epithelial cells to respond with a range of cytokines like TGF- $\alpha$  and CXCL8 (Gomez *et al.*, 2006; Quinn and Cole, 2007; Saba *et al.*, 2006).

Intracellular receptors, linked to IFN, can also recognize staphylococci in the airway, since the epithelial cells internalize some bacterial components. It is known that type I IFN signaling is an important viral defense pathway in the lung resulting in expression of several ISGs, and *S. aureus* also activates this pathway (Martin and Parker *et al.*, 2011; Soong *et al.*, 2011). The bacteria activate type I IFN signaling through several TLRs, NLRs and other receptors that sense cell wall components, DNA and RNA (Charrel-Denis *et al.*, 2008). This will lead to the IFN- $\beta$  production via phosphorylation of IFRs, like IFR3, 5 and 7. As explained in section 1.2, IFN- $\beta$  interacts with IFNAR, activating JAK-STAT pathway. Then STAT1 and 2 binds with IRF9 and form ISGF3, which will lead to the transcription of several ISGs, like the *Mx-1* and *Lif* (Martin FJ, *et al.*, 2009).

Another known cause of pulmonary pathology is the IL-1 $\beta$  and the IL-18 cytokines, which are a major component of the inflammasome. IL-1 $\beta$  is produced in response to TLR2 recognition and membrane perturbation by  $\alpha$ -hemolysin, leading to production of active caspase-1 that cleaves pro-IL-1 $\beta$  to enable secretion of mature IL-1 $\beta$  (Bergsbaken, 2009). Concomitantly, pyroptosis, a highly inflammatory form of cell death is induced (Munoz-Planillo, 2009; Lappalainen and Whitsett, 2005). Pyroptosis is due to the activation of the inflammasome, characterized by the activation of caspase-1 and production of IL-1 $\beta$  and IL-18 (Martinon, 2002). *S. aureus* components that activate the production of IL-1 $\beta$  is peptidoglycan and cell wall degradation products (Shimada *et al.*, 2010) The cytokines generated in response to the

activation of the inflammasome are likely to contribute to pulmonary pathology (Parker and Prince 2013).

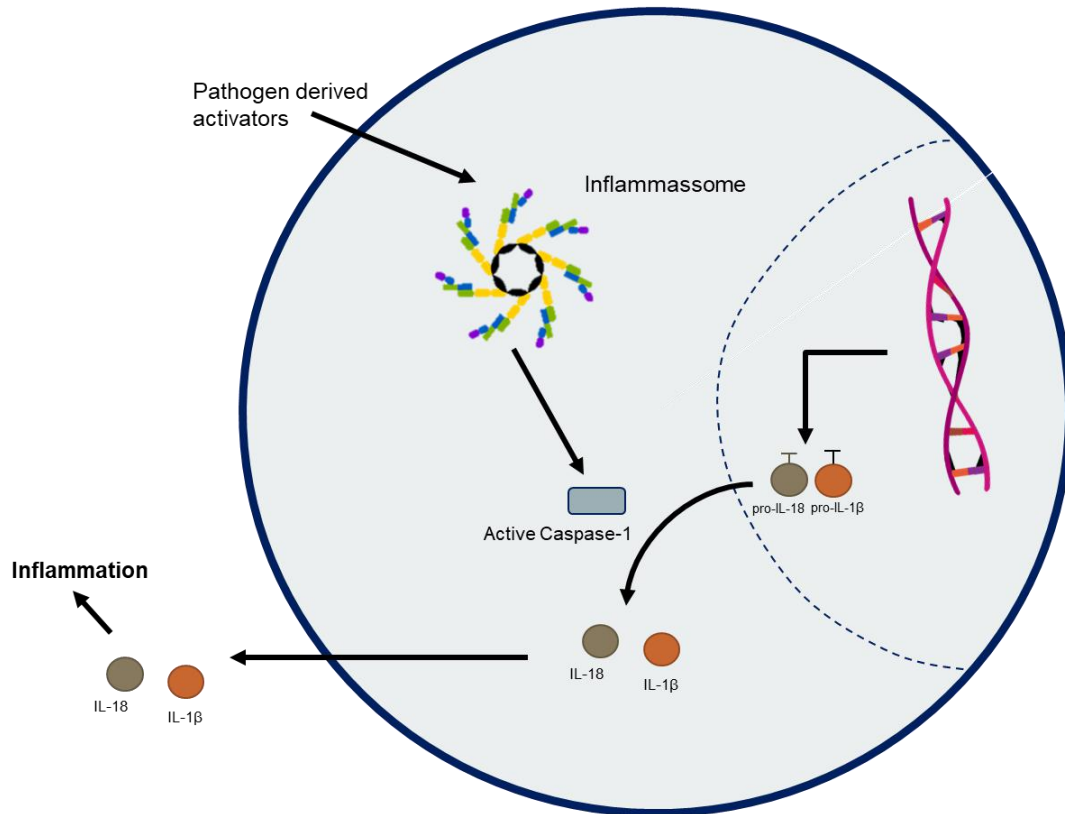


**Figure 4 – Inflammasome activation leading to production of IL-18 and IL-1 $\beta$  cytokines.**

### **1.5. IAV and *S. aureus* infection**

Interactions between IV and *S. aureus* in the pathogenesis of respiratory infections have been reported since many decades. While IV infections sometimes result in fatal cases, co-infections increase drastically the mortality rates (Bosch *et al.*, 2013). *S. aureus*, *Streptococcus pneumoniae* (*S. pneumoniae*) and *Haemophilus influenzae* (*H. influenzae*) are the most common pathogens associated with such secondary infections. They occur frequently but are of major importance during influenza pandemics.

The most well-known case is the 1918-1919 “Spanish flu”, where 50 million of lives were lost, most from pneumococcal pneumonia (McCullers, 2006). During the remain of the 20<sup>th</sup> century and in the 21<sup>th</sup> other influenza pandemics were reported: in 1957-1958 the “Asian flu”, in 1968-1969 the

“Hong Kong flu” and more recently, in 2009 the “Swine flu” pandemic. During these pandemics, many cases of bacterial co-infections were observed (Morens *et al.*, 2008). *S. pneumoniae* is associated with high mortality during influenza epidemics and pandemics (Brundage, 2006). It was responsible for most of the deaths during the 1918-1919 pandemic (Brundage and Shanks, 2008, Morens *et al.*, 2008). However, *S. aureus* has an increasing importance as a secondary pathogen due to the emergence of community acquired MRSA strains and its predominance during the later pandemics and interpandemic times (Morens *et al.*, 2008).

### **1.6. Pathogenesis of co-infection**

Establishment of clinical co-pathogenesis requires the interaction of bacteria, viruses and their host. The complex interplay of cellular, bacterial and viral factors that lead to secondary bacterial infections, following primary viral exposure, have been extensively investigated. Particularly the co-pathogenesis of influenza viruses with bacterial infections was in focus of interest. However, possible consequences of a primary bacterial exposure, like in acute or chronic infections, but also as part of the microbiome, for secondary viral infections are less understood (Bellinghausen, 2016). So far it is known that viral factors, such as the NA cleaves respiratory epithelial cells sialic acids, contributing to increased bacterial adhesion and dissemination (McCullers, 2003, Peltola *et al.*, 2005). Similarly, the tissue damage due to IV infection contributes to increased adherence and infection efficiency by the bacteria (Iverson *et al.*, 2011). In addition to the NA, the viral PB1-F2, an apoptosis inducer, increases the susceptibility to bacterial co-infection (McAuley, 2007).

Moreover, upon a co-infection the host immune response is often dysregulated, the activity of immune cells is decreased and there is a reduction of mucociliary clearance, resulting in an increased pathogen burden (Vareille *et al.*, 2011). Nonetheless, bacterial factors, such as the PVL toxin, that increase inflammation are of major importance, too. In consequence all these interactions contribute to pathogenicity and often lead to manifestation of systemic infections.

### 1.7. Influence of prior bacterial exposure upon viral infection

The notion of a balanced, beneficial and healthy microbiome is well established for the gastrointestinal tract, where bacteria aid by competing against potential harmful micro-organisms and synthesize molecules like vitamins (Kamada *et al.*, 2013). Also, commensal bacteria shape intestinal immune responses in both health and disease (Hooper *et al.*, 2012; Chervonsky, 2010). The same beneficial effects of a pulmonary microbiome could shape the immune response to a subsequent infection (Bellinghausen, 2016). Since airway damage due to viral infection is caused mainly by severe inflammation, a healthy microbiome, might help controlling the tissue damage. It has been shown that existence of commensal bacteria in the upper respiratory tract reduce acute lung damage induced by influenza. Furthermore, it was shown that mortality in mice is reduced by recruitment of monocytes into the lungs (Wang *et al.*, 2017). Another study revealed that there is a connection between the commensal microbiome and inflammasome-dependent cytokine activation, although the mechanism behind it is not well known (Chen *et al.*, 2016). One hypothesis is that products from a determined group of commensal bacteria may trigger PRRs which will stimulate leukocytes. Then products released by these leukocytes support production of pro-IL-1 $\beta$ , pro-IL-18 and others for inflammasome-dependent cytokine activation (Ichinohe, 2011).

However, in another way, exposure to pathogenic bacteria, during chronic diseases, might negatively affect a consequent viral exposure. Several studies have reported a persistent presence of potential pathogenic micro-organisms during this type of diseases. There are some examples from the interplay of bacteria, like *H. influenzae*, and respiratory viruses as a model. In 25 % of all patients suffering from chronic obstructive pulmonary disease (COPD), *H. influenzae* is commonly found in their lungs, during stable periods of the illness (Cabello *et al.*, 1997, Zalacain *et al.*, 1999; Monsó *et al.*, 1999). It was also shown that the expression of ICAM-I is increased in respiratory epithelial cells upon exposure to *H. influenzae*, which is a main receptor for human rhinovirus (HRV). This translates in increased viral binding and

replication of these virus *in vitro* (Gulraiz *et al.*, 2015, Saijan *et al.*, 2006). *H. influenzae* can also work together with respiratory syncytial virus (RSV) and induce the production of pro-inflammatory cytokines (Bellinghausen, 2016). *Moraxella catarrhalis*, which is also commonly present in the lower respiratory tract of COPD patients, has been shown to impair TLR3 expression in bronchial epithelial cells. Decrease in TLR3, leads to less recognition of viral structures and antiviral type I/III IFN production (Heinrich *et al.*, 2016).

Factors that make patients more susceptible to both types of pathogens (viruses and bacteria), compromised immune functions, or up-regulation of viral entry receptors, but also synergistic effects on inflammation or tissue damage might explain the co-pathogenesis of chronic bacterial exposure followed by acute viral infections (Bellinghausen, 2016). However, the studies on these subjects are still limited.

### **1.8. Study aims**

IV are a high health risk. It affects mainly children, elderly and immunosuppressed patients. Influenza infections are often associated with more severe complications due to bacterial co-infections. The complex interactions and mechanisms of cellular, bacterial, and viral factors that lead to secondary bacterial infections have been well investigated. However, the effects that a primary bacterial exposure, due to the presence of a healthy microbiome, or to the existence of acute or chronic infections, can cause on a secondary viral infection are not well understood. It is known that a healthy microbiome, like in the intestinal tract, aid us fighting unwanted pathogens, and the same benefit could be present in the lung's microbiome. However, it is also known that exposure to pathogenic bacteria, like in chronic diseases, bring negative effects during a consequent viral exposure as shown in other studies. Thus, the goal, of this study was to develop an infection model that could mimic a primary bacterial exposure and its effects on a consequent viral infection. The main goal was then to observe if the primary bacterial exposure would prime the cells to a subsequent viral infection or if the development of tolerance or resistance would take place. The study was performed with IV, and with a

pathogenic strain of *S. aureus* due to the importance of this bacterium as a rising cause of co-infections together with these viruses and due to the emergence of resistant strains, like MRSA. During this study, an infection protocol that can mimic a primary bacterial exposure had to be established and the effects of primary exposure to pathogenic bacteria on secondary viral infections were analyzed.

## 2. Material

### 2.1. Equipment and material

Denomination	Manufacturer
Accu-jet® pro	Brand GmbH (Wertheim, Germany)
Analytical Balance	Sartorius (Göttingen, Germany)
BioPhotometer	Eppendorf (Hamburg, Germany)
Blot Chamber	BioRad (Munich, Germany)
Canon EOS 500D Camera	Canon (Krefeld, Germany)
Centrifuge 5417R and 5810R	Eppendorf (Hamburg, Germany)
CO <sub>2</sub> -Incubator (used for infection)	Eppendorf (Hamburg, Germany)
Colony Counter ProtoCOL 3 Plus	Synoptics Ltd. (Cambridge, UK)
Costar® Pipette (2mL; 5mL; 10mL; 25mL)	Corning Incorporated (Corning, New York, USA)
Cuvettes (Plastic)	Sarstedt (Nümbrecht, Germany)
Eppendorf Safe-Lock Tubes	Eppendorf (Hamburg, Germany)
FACSCalibur™	BDBiosciences (Heidelberg, Germany)
Falcon Tubes (15mL; 50 mL)	Greiner Bio-One (Frickenhäusen, Germany)
Filters (Ø = 0.2/0.45 µm)	GE Healthcare Europe GmbH (Freiburg, Germany)
Fridge (4 °C)	Liebherr-International Deutschland GmbH (Ochsenhausen, Germany)
Freezer (-80 °C) MFD-DU500VH-PE Ultra Low Freezer	Panasonic Biomedical Sales (Hamburg, Germany)
Freezer and Fridge Herafreeze	Heraeus (Hanau, Germany)
Gel Eletrophoresis device	BioRad (Munich, Germany)

Heating Block	NORAS Röntgen u. Medizintechnik GmbH Nunc (Roskilde, Denmark)
Imaging System Odyssey Fc (CCD camera system)	LI-COR Biosciences (Bad Homburg, Germany)
Incubator (used for cell culture) MCO-20AIC	Sanyo (Bad Nenndorf, Germany)
Incubator (used for co-infection) new Brunswick Galaxy 48R	Eppendorf AG (Hamburg, Germany)
Inverse Microscope Axiovert 40C	Zeiss (Jena, Germany)
Laboratory pH-meter 765 Calimatic	Knick (Berlin, Germany)
Nanodrop NP-100	PEQLAB Biotechnology (Erlangen, Germany)
Pipette (10 µL; 20 µL; 100 µL; 1000 µL)	Eppendorf AG (Hamburg, Germany)
Pipette tips (10 µL; 20 µL; 100 µL; 1000 µL)	Sarstedt (Nümbrecht, Germany)
Plastic tubes (10 mL)	Sarstedt (Nümbrecht, Germany)
Power-Pac™ Basic 300 Power Supply	BioRad (Munich, Germany)
PROTRAN Nitrocellulose Transfer Membrane	Schleicher & Schüll (Dassel, Germany)
Reaction Tubes (1.5 mL; 2 mL)	Eppendorf AG (Hamburg, Germany)
Roche Light Cycler 480 II	Fa. Hoffman-La Roche (Basel, Switzerland)
Multiwell plate 96 (qRT-PCR)	Greiner Bio-One (Frickenhäusen, Germany)
SafeSeal-Tips professional (10 µL; 20 µL; 200 µL; 1000 µL)	Biozym Scientific GmbH (Hessisch, Oldendorf, Germany)
Shaker Heidolph Duomax 1030	Heidolph Instruments GmbH & Co.

Spectramax M2	KG Molecular Devices (Sunnyvale, CA, USA)
Sterile bench (used for cell culture)	BDK (Sonnenbühl-Genkingen, Germany)
Syringe (1, 20 mL)	Becton, Dickinson & Co. (Heidelberg, Germany)
Thermomixer Comfort	Eppendorf (Hamburg, Germany)
Whatman GB002 paper	Schleicher & Schüll (Dassel, Germany)

## 2.2. Software

Denomination	Manufacturer
SoftMax <sup>®</sup> Pro 6	Molecular Devices (Sunnyvale, CA, USA)
Image Studio Lite (V5.2.5)	LI-COR Biosciences (Bad Homburg, Germany)
BD CellQuest <sup>™</sup> Pro (V5.2)	BD Biosciences (Heidelberg, Germany)
ND-1000 (V3.5.2)	PeqLab (Erlangen, Germany)
ProtoCOL 3 (V1.1.0.0)	Synoptics Ltd. (Cambridge, UK)
GraphPad Prism <sup>®</sup> (V6)	GraphPad Software, Inc. (La Jolla, CA, USA)
Light Cycler <sup>®</sup> 480 Software (V1.5.1)	Fa. Hoffmann-La Roche (Basel, Switzerland)

## 2.3. Chemicals and reagents

Denomination	Manufacturer
β-2-mercaptoethanol	Roth (Karlsruhe, Germany)
2-Propanol	Roth (Karlsruhe, Germany)

Acrylamide	Serva (Heidelberg, Germany)
Agar	Oxoid (Basingstoke, UK)
Ammonium Persulfate (APS)	Roth (Karlsruhe, Germany)
Aprotinin	Roth (Karlsruhe, Germany)
Bacto™ Agar	BD Biosciences (Heidelberg, Germany)
Benzamidine	Sigma-Aldrich (Munich, Germany)
Bromophenol Blue	Sigma-Aldrich (Munich, Germany)
Calcium Chloride (CaCl <sub>2</sub> )	Roth (Karlsruhe, Germany)
Diethylaminoethyl-dextran (DEAE-Dextran)	Sigma-Aldrich (Munich)
Ethylenediamin-tetra-acetic acid (EDTA)	Roth (Karlsruhe, Germany)
Ethanol, 96%	Roth (Karlsruhe, Germany)
Glycerol	Roth (Karlsruhe, Germany)
Glycin	Roth (Karlsruhe, Germany)
Hydrochloric acid (HCl)	AppliChem (Darmstadt, Germany)
Hydrogen peroxide (H <sub>2</sub> O <sub>2</sub> )	Roth (Karlsruhe, Germany)
Leupeptin	Serva (Heidelberg, Germany)
Luminol	Sigma-Aldrich (Munich, Germany)
Magnesium chloride (MgCl <sub>2</sub> )	Roth (Karlsruhe, Germany)
Methanol	Roth (Karlsruhe, Germany)
Milk powder	AppliChem (Darmstadt, Germany)
PageRuler™ prestained protein ladder	Fermentas (St. Leon-Rot, Germany)
Phosphate buffered saline (PBS) 1x	Sigma-Aldrich (Munich, Germany)
p-coumaric acid	Sigma-Aldrich (Munich, Germany)
Pefablock	Roth (Karlsruhe, Germany)
Reaction Buffer (5x) for H minus	Thermo Fischer Scientific (Karlsruhe, Germany)
Reverse Transcriptase (RT)	Thermo Fischer Scientific
Revert Aid H minus RT	

	(Karlsruhe, Germany)
Tetramethylethylenediamine (TEMED)	Roth (Karlsruhe, Germany)
Tris(hydroxymethyl)aminomethane (TRIS)	Roth (Karlsruhe, Germany)
Trypan Blue	Gibco Invitrogen (Karlsruhe, Germany)
Tween® 20	Roth (Karlsruhe, Germany)
Sodium chloride (NaCl)	Roth (Karlsruhe, Germany)
Sodium dodecyl sulfate (SDS)	Roth (Karlsruhe, Germany)
Sodium orthovanadate	Sigma-Aldrich (Munich, Germany)

## 2.4. Nutrients and additives

Denomination	Manufacturer
Bovine serum albumin (BSA, 35%)	MP Biomedicals (Eschewege, Germany)
Brain heart infusion medium (BHI)	Merck (Darmstadt, Germany)
Dulbecco Modified Eagle Medium (DMEM) high Glucose (+ L-Glutamine)	Sigma-Aldrich (Munich, Germany)
Fetal calf serum (FCS)	Biochrom AG (Berlin, Germany)
Gentamicin	Sigma-Aldrich (Munich, Germany)
4-(2-hydroxyethyl)-1-piperazineethanesulfonic acid (HEPES)	Gibco Invitrogen (Karlsruhe, Germany)
Human serum albumin (20%)	CLS Behring (Marburg, Germany)
Lysostaphin	Sigma-Aldrich (Munich, Germany)
Modified Eagle Medium (MEM) high Glucose (+ L-Glutamin)	Sigma-Aldrich (Munich, Germany)
MEM 10×	Gibco Invitrogen (Karlsruhe, Germany)

Neutral Red	Sigma-Aldrich (Munich, Germany)
Penicillin/Streptomycin	PAA Laboratories (Pasching, Germany)
Trypsin-EDTA	Gibco Invitrogen (Karlsruhe, Germany)
Trypsin-TPCK (treated with L-tosylamide-2-phenylethyl chloromethyl ketone (TPCK))	Gibco Invitrogen (Karlsruhe, Germany)

## 2.5. Material for cell culture

Denomination	Manufacturer
Blood agar plate (Sheep)	Oxoid (Basingstoke, UK)
Cell culture dishes (15 cm)	Greiner Bio-One (Frickenhausen, Germany)
Cell culture flasks (T75)	Greiner Bio-One (Frickenhausen, Germany)
Cell culture multi well plates (6-well; 12-well; 96-well)	Greiner Bio-One (Frickenhausen, Germany)
Cell scraper	Sarstedt (Nümbrecht, Germany)
Hemocytometer	Merck (Darmstadt, Germany)
Inoculation loops	Nunc (Roskilde, Denmark)
Sterile pipettes (2, 5, 10, 25 mL)	Corning Life Science (USA)

## 2.6. Medium and buffers

Denomination	Manufacturer
Blocking solution (for Western Blot)	5% (w/v) skim milk powder in TBS-Tween (1×)
Blot-buffer	192 mM Glycin 25 mM Tris 15% (v/v) Methanol in ddH <sub>2</sub> O

BHI Agar	37 g BHI medium 18 - 20 g Bacto™ Agar in 1 L ddH <sub>2</sub> O
BHI medium	37 g in 1 L ddH <sub>2</sub> O Autoclaved before use
DMEM	add 10% FCS
Infection medium (used for cell culture)	1 mM MgCl <sub>2</sub> 0.9 mM CaCl <sub>2</sub> 100 U/mL Penicillin 0.1mg/mL Streptomycin 0.2% BSA
ECL-reagent	2.5 mM Luminol 0.36 mM p-cumar acid 100 mM Tris-HCl pH 8.5 0.01% H <sub>2</sub> O <sub>2</sub> (add before use)
Infection-PBS	1 mM MgCl <sub>2</sub> 0.9 mM CaCl <sub>2</sub> 100 U/mL Penicillin 0.1 mg/mL Streptomycin 0.2% BSA in PBS
Infection medium (used for co-infection)	0.21% (w/v) BSA 0.01% (w/v) Ca <sup>2+</sup> /Mg <sup>2+</sup> in DMEM
Invasion medium (used for co-infection)	0.2% (v/v) HSA 1 mM HEPES in DMEM
MEM	add before use 10% FCS
MEM (1.5×)	50 mL 10× MEM 276 mL ddH <sub>2</sub> O

	100 U/mL Penicillin 0.1 mg/mL Streptomycin 14 mL Na (CO <sub>3</sub> ) <sub>2</sub> 5 mL 1% DEAE Dextran 0.2 % BSA autoclaved before used
Oxoid-Agar	3% (w/v) Oxoid-Agar in ddH <sub>2</sub> O autoclaved before used
Plaque medium	70% (v/v) 1.5× MEM 0.9% (w/v) Oxoid-Agar 0.01% (w/v) Ca <sup>2+</sup> /Mg <sup>2+</sup> 0.12% Trypsin TPCK
RIPA buffer	25 mM Tris/HCl pH 8 137 mM NaCl 10 % (v/v) Glycerol 0.1 % (w/v) SDS 0.5 % (w/v) DOC 1 % (v/v) NP-40 2 mM EDTA pH 8 in ddH <sub>2</sub> O  add before use: 0.2 mM Pefablock 5 µg/mL Aprotinin 5 µg/mL Leupeptin 5 mM Benzamidine 1 mM Sodium orthovanadate
SDS-page running buffer (5×)	25 mM Tris 250 mM Glycin 0.1% (w/v) SDS in ddH <sub>2</sub> O
SDS-page sample	10% (w/v) SDS

buffer (5×)	50% (v/v) Glycerin 25% (v/v) β-Mercaptoethanol 0.1% (v/v) Bromophenol blue 312 mM Tris/HCl pH 6.8 in ddH <sub>2</sub> O
SDS-page stacking gel	178 mM Tris/HCl 1% (v/v) TEMED 0.1% (w/v) SDS 0.1% (w/v) APS 1% (v/v) Acrylamide in ddH <sub>2</sub> O
SDS-page running gel	370 mM Tris/HCl pH 8.9 0.02% (v/v) TEMED 0.1% (w/v) SDS 0.1% (w/v) APS 7.5% (v/v) Acrylamide in ddH <sub>2</sub> O
Stop medium	10% (v/v) FCS 0.1 mg/mL Gentamicin / 2 µg/mL Lysostaphin in DMEM
TBS-Tween (20×) (TBS-T)	50 mM Tris pH 7.4 150 mM NaCl 0.05% (v/v) Tween20 in ddH <sub>2</sub> O

## 2.7. Kits

Denomination	Manufacturer
Brilliant III® SYBR Green QPCR Master Mix	Agilent (Waldbronn, Germany)
CytoSelect™ LDH Cytotoxicity Assay Kit	Cell Biolabs (San Diego, CA, USA)

LEGENDplex™ Human Inflammation Panel (13-plex) RNeasy Plus Mini Kit	BioLegend® (San Diego, CA, USA) Qiagen (Hilden, Germany)
---	--

## 2.8. Primer

### 2.8.1. Primers for qRT-PCR

Sequences of the forward (*fwd*) and reverse (*rev*) Primers used

Denomination	Sequence (5'-3')	Manufacturer
<i>GAPDH fwd</i>	GCCAATTCCATGGCACCCT	Eurofins Genomics (Ebersberg, Germany)
<i>GAPDH rev</i>	GCCCCACTTGATTTTGGAG G	
<i>IFNβ fwd</i>	TCTGGCACAACAGGTAGTA GGC	Eurofins Genomics (Ebersberg, Germany)
<i>IFNβ rev</i>	GAGAAGCACAACAGGAGAG CAA	
<i>IL-6 fwd</i>	TCTGGCTTGTTCTCACTAG T	Eurofins Genomics (Ebersberg, Germany)
<i>IL-6 rev</i>	AACCTGAACCTTCCAAAGAT GG	
<i>IL-8 fwd</i>	CTTGTTCCACTGTGCCTTGG TT	Eurofins Genomics (Ebersberg, Germany)
<i>IL-8 rev</i>	GCTTCCACATGTCCTCACAA CAT	
<i>IL-18 fwd</i>	TTCAACTCTCTCCTGTGAGA ACA	Eurofins Genomics (Ebersberg, Germany)
<i>IL-18 rev</i>	AGAVAAAAGGTTGGTCTGA GGA	
<i>IP-10 fwd</i>	GGAACCTCCAGTCTCAGCA CCA	Eurofins Genomics (Ebersberg, Germany)
<i>IP-10 rev</i>	AGACATCTCTTCTCACCTT	

<i>MDA5 fwd</i>	C	Eurofins Genomics (Ebersberg, Germany)
<i>MDA5 rev</i>	TGCAGTGTGCTAGCCTGTT	
	C	Eurofins Genomics (Ebersberg, Germany)
	TAAGCCTTTGTGCACCATCA	
<i>MxA fwd</i>	GTTTCCGAAGTGGACATCG	Eurofins Genomics (Ebersberg, Germany)
<i>MxA rev</i>	CA	
	GAAGGGCAACTCCTGACAG	Eurofins Genomics (Ebersberg, Germany)
	T	
<i>M1 fwd</i>	TGCAAAAACATCTTCAAGTC	Eurofins Genomics (Ebersberg, Germany)
<i>M1 rev</i>	TCTG	
	AGATGAGTCTTCTAACCGAG	Eurofins Genomics (Ebersberg, Germany)
	GTCG	
<i>OAS1 fwd</i>	GATCTCAGAAATACCCCAG	Eurofins Genomics (Ebersberg, Germany)
<i>OAS1 rev</i>	CA	
	AGCTACCTCGGAAGCACCT	Eurofins Genomics (Ebersberg, Germany)
	T	
<i>PB1 fwd</i>	CATACAGAAGACCAGTCGG	Eurofins Genomics (Ebersberg, Germany)
<i>PB1 rev</i>	GAT	
	GTCTGAGCTCTTCAATGGTG	Eurofins Genomics (Ebersberg, Germany)
	GA	
<i>RIG-I fwd</i>	CCTACCTACATCCTGAGCTA	Eurofins Genomics (Ebersberg, Germany)
<i>RIG-I rev</i>	CAT	
	TCTAGGGCATCCAAAAAGC	Eurofins Genomics (Ebersberg, Germany)
	CA	

### 2.8.2. Other Oligonucleotides

Denomination	Sequence (5'-3')	Manufacturer
Oligo-(dT)	TTT TTT TTT TTT TTT T	Eurofins Operon (Ebersberg, Germany)

## 2.9. Antibodies

### 2.9.1. Primary Antibodies

Denomination	Species	Dilution	Manufacturer
Influenza A PB1	Rabbit	1:1000	Gene Tex (Irvine, CA, USA)
Peptidoglycan	Mouse	1:500	BioRad (Munich, Germany)
Phospo-p42/p44 T202/Y204 (pERK1/2)	Mouse	1:1000	Cell Signalling Technologies (Frankfurt, Germany)
Phospo-STAT1 (Y701) (D407)	Rabbit	1:1000	Cell Signalling Technologies (Frankfurt, Germany)
p42/p44 MAP Kinase (ERK1/2)	Mouse	1:1000	Cell Signalling Technologies (Frankfurt, Germany)
STAT1	Mouse	1:1000	BD Biosciences (Heidelberg, Germany)

### 2.9.2. Secondary Antibodies

Denomination	Dilution	Manufacturer
IRDye® 800CW donkey <i>anti-mouse</i> IgG (H+L)	1:10000	LI-COR Biosciences (USA)
IRDye® 800CW donkey	1:10000	LI-COR Biosciences

<i>anti-rabbit</i> IgG (H+L)		(USA)
IRDye® 680RD Donkey <i>anti-rabbit</i> IgG (H+L)	1:10000	LI-COR Biosciences (USA)
IRDye® 680RD donkey <i>anti-mouse</i> IgG (H+L)	1:10000	LI-COR Biosciences (USA)
Horse <i>anti-mouse</i> IgG- horseradish-peroxidase (HRP)	1:3000	Cell Signalling Technologies (Frankfurt, Germany)
Horse <i>anti-rabbit</i> IgG- HRP	1:3000	Cell Signalling Technologies (Frankfurt, Germany)

## 2.10. Cell lines

Denomination	Description	Culture medium
A549	Human Alveolar Basal Epithelium Cells	DMEM + 10% FCS
Madin-Darby canine kidney (MDCK II)	Dog Renal Epithelial Cells	MEM + 10% FCS

## 2.11. Pathogens

### 2.11.1. Virus

Denomination	Description	Reference
A/Puerto Rico/8/34 (H1N1) (PR8M)	Human Influenza A virus isolate	(Liedmann <i>et al.</i> , 2014)

### 2.11.2. Bacteria

Denomination	Manufacturer	Reference
<i>S. aureus</i> 6850 wt	Isolate from a patient with Osteomyelitis, wildtype (wt)	GenBank ATCC536657

### **3. Methods**

#### **3.1. Cell culture**

All the cell culture work was done under sterile conditions with endotoxin-free materials in a level II sterile workbench. All cells were cultivated in an incubator in a humidified atmosphere at 37°C and 5% CO<sub>2</sub>.

A549 cells were cultivated in DMEM, while MDCKII cells were cultivated in MEM. Both media were supplemented with 10 % (v/v) FCS.

When the cells reached a confluence of 70 – 90 %, cells were washed with PBS and detached with 3 mL of pre-warmed Trypsin-EDTA solution. Cells were incubated at 37 °C until the monolayer was completely detached and then resuspended with 7 ml fresh medium. For subcultivation, cells were divided into cell culture dishes (15 cm) or flasks (75 / 175 cm<sup>2</sup>). For the realization of the experiments, cells were counted and seeded with  $0.2 \times 10^6$  or  $0.5 \times 10^6$ , in 12-well or 6-well plates, respectively.

#### **3.2. Virological methods**

Influenza virus [A/Puerto Rico/8/34 (H1N1) (PR8M)] used in the present study is a human isolate of risk group 2 and was accordingly handled in laboratories of safety level 2 and stored there at -80 °C. All steps involving infectious viruses were performed using a biosafety cabinet.

##### **3.2.1. Virus propagation**

For IAV propagation, MDCK II cells were seeded into 15 cm cell culture dishes and infected when the cell monolayer presented a confluence of around 80 - 90 %. The cells were washed once with 10 mL of PBS. Subsequently, 13 mL of MEM infection medium was added, supplemented with TPCK-Trypsin (1 mg/mL). Virus stocks were diluted in 20 mL of infection PBS at a multiplicity of infection (MOI) of 0.0001 and added to the medium. The cells were incubated for 48 or 72 h. When a cytopathogenic effect was visible, supernatants were harvested, and cell debris was removed by centrifugation for 10 min at 3226 rcf

at 4 °C. Supernatants were aliquoted in sterile tubes and stored at – 80 °C until further use. Virus titers were determined by standard plaque assay (see section 3.2.2).

### **3.2.2. Determination of infectious virus titres (standard plaque assay)**

The detection of infectious virus particles was achieved indirectly through the detection of a plaque formation, represented by holes in the cell layer caused by the lytic viral infection.

For this technique, a nearly confluent 15 cm dish of MDCK II cells was used to seed two 6-well plates (2 mL per well), one day before the plaque assay performed, to generate a confluent cell layer.

The samples were serially diluted 1:10 in infection PBS. Cells were rinsed with PBS and 500 µL sample dilution were added. Thereafter, cells were incubated at 37 °C, being agitated every 10 min. After 30 min the virus solution was aspirated, the cells were supplemented with 2 mL of pre-warmed plaque medium, containing 0.9 % liquid agar, and were incubated, upside-down, at 37 °C for 2 - 3 days until plaques were visible. The agar overlay avoids the diffusion of the released progeny virus particles, restricting the infection to only directly neighboring cells, until, after multiple infection cycles, a pale plaque becomes visible. This way, a plaque corresponds to one initial virus particle infecting a cell. Cell layers were then stained with neutral red in PBS, plaques were counted, and viral titers determined using the following formula:

$$\text{Virus titer (PFU mL}^{-1}\text{)} = \text{Number of plaques} \times \text{dilution level} \times 2$$

### **3.3. Bacteriological methods**

*S. aureus* was stored on blood agar plates at 4 °C. Every four weeks, fresh blood agar plates were inoculated with bacteria stored in 30 % glycerol at - 80 °C.

### 3.3.1. Cultivation

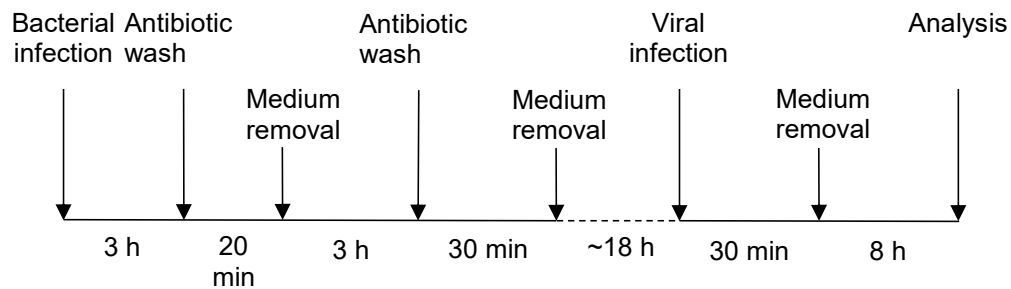
For each experiment, a fresh overnight culture (ONC) was prepared the day before. For this, 5 mL of BHI medium were inoculated with a single *S. aureus* colony taken from the blood agar plate and incubated at 37 °C for 16 h without shaking. Before the start of the experiment, the cells were pelleted by centrifugation for 5 min at 3226 rcf, 4 °C, washed once with 5 mL of PBS, centrifuged again and then resuspended in approximately 9.8 mL of PBS. The number of bacteria was measured by determining the optical density (OD) at 600 nm. Previously, for the *S. aureus* 6850 strain an OD<sub>600nm</sub> = 1 was determined to represent a viable bacterial count of 5×10<sup>8</sup> Colony Forming Units (CFU) mL<sup>-1</sup>. For infection of cells, the bacterial suspension was then adjusted to the desired MOI in invasion medium.

### 3.3.2. Determination of colony-forming bacterial titers

To quantify extracellular bacteria, A549 cells were infected, as described in section 3.4.1, and at 32 or 48 h post-infection (p.i.) supernatants were collected, serially diluted in PBS and 50 µL were plated on BHI-agar plates. After overnight incubation at 37 °C, colonies were counted, and the viable bacterial titer calculated using the following formula:

$$\text{Number of colonies} \times \text{dilution level} \times 20 = \text{CFU mL}^{-1}$$

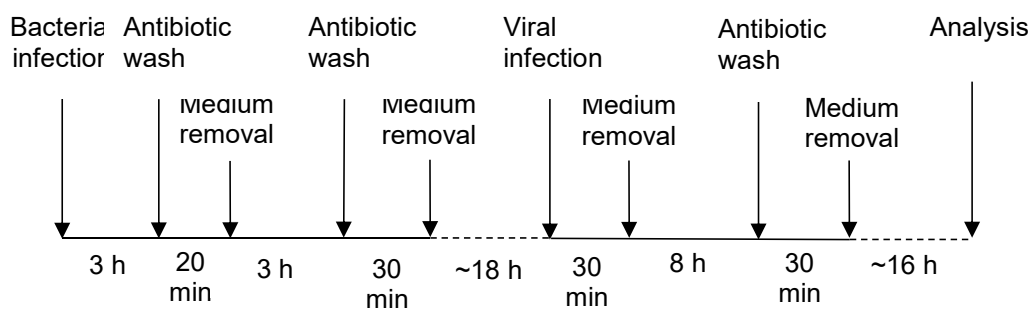
To determine intracellular bacteria, the cells were washed with PBS and incubated at 37 °C with stop medium containing 2 µg mL<sup>-1</sup> lysostaphin to remove the non-internalized bacteria for 20 min. Then the cells were washed twice with PBS and incubated for 0.5 h with 2 mL of ddH<sub>2</sub>O at 37 °C to lyse the cells by osmotic shock. The lysates were transferred to plastic tubes (10 mL), centrifuged for 10 min at 3226 rcf, 4 °C and resuspended in 1 mL PBS. Samples were serially diluted and then 50 µL were used to inoculate BHI-agar plates. After overnight incubation at 37 °C, colonies were counted, and the bacterial titers determined.



### 3.4. Co-infection model

Figure 5 - 32 and 48 hours infection scheme of a secondary viral infection after primary *S. aureus* infection.

#### 3.4.1. Infection with *S. aureus* and IAV



A549 cells were seeded in 6-well plates ( $A549 - 0.5 \times 10^6$ ) in 2 mL of culture medium (DMEM) or in 12-well plates ( $A549 - 0.25 \times 10^6$ ) in 1 mL of culture medium 18 h before the start of the experiment. The supernatant was aspirated, the cells were washed with PBS and then incubated with 0.001 MOI *S. aureus* 6850 wt in 1 mL (6-well plates) or 500  $\mu$ L (12-well plates) of invasion medium (DMEM/INV) for 3 h at 37 °C. To prevent the overgrowth of extracellular bacteria, antibiotic washes were performed at 3, 6 h post infection (p.i.). The first antibiotic wash at 3 h p.i. was performed with lysostaphin. Therefore, medium was aspirated, cells were washed with PBS and incubated with 1 mL of stop medium supplemented with 2  $\mu$ g mL<sup>-1</sup> lysostaphin (6-well plates) or with 500  $\mu$ L (12-well plates) for 20 min at 37 °C. Subsequently, the medium was removed, the cells washed with PBS and incubated in 1 mL or

500  $\mu$ L of infection medium (DMEM/INF) at 37 °C. At 6 h p.i., supernatant was withdrawn, the cells were washed with PBS and incubated for 0.5 h at 37 °C with 1 mL of stop medium supplemented with 100  $\mu$ g mL<sup>-1</sup> gentamicin. Again, cells were washed and further incubated until 24 h p.i. at 37 °C. Then, the supernatant was aspirated, the cells were washed with PBS and incubated with IAV of MOI 1 (8 h infection), or with MOI of 0.1 or 0.5 (24 h infection) in 500  $\mu$ L (6-well plate) or 250  $\mu$ L (12-well plate) in infection medium for 0.5 h at 37 °C. The supernatant was then removed, the cells were washed and incubated with 1 mL (6-well plate) or 500  $\mu$ L (12-well plate) of infection medium at 37 °C for 8 h. At this time all the subsequent analyses were performed, or in case of a long-term viral infection (48 h), a third antibiotic wash with lysostaphin was included, according to procedure as described before. After this step the cells were further incubated until 24 h p.i..

Alternatively, the supernatants were transferred to Eppendorf reaction tubes, centrifuged at 20817 rcf for 2 min to remove extracellular bacteria without removal of infectious viral particles and secreted cytokines and chemokines in the medium. Afterwards, the medium was transferred back to the corresponding wells until the end of the experiment.

The difference between the washing times are due to the antibiotics used. Shorter times were used for a lysostaphin wash, in contrast to a gentamicin wash, since the first one is more aggressive than the second, and additional cell stress should be avoided.

### **3.5. Molecular biological methods**

#### **3.5.1. Nucleic acids**

##### **3.5.1.1. RNA extraction**

To isolate total RNA from uninfected or infected A549 cells, lysis was performed by addition of RLT plus lysis buffer supplemented with 1 % (v/v) 2-mercapthoethanol (350  $\mu$ L per well (12-well plates)). Lysates were then stored at – 80 °C or directly used for isolation of total RNA using the RNeasy Plus Mini Kit (Qiagen) according to the manufacturer's instruction. Briefly, during the first step genomic DNA binds to a column, then the flow through is mixed with

Ethanol and transferred to a second spin column and placed in the centrifuge. The centrifuge forces the solution through a silica gel membrane placed in the column, binding the RNA, allowing isolation and purification. The final elution step was done with 30  $\mu$ L of RNase-free water supplied with the kit. The isolated RNA was then stored at  $-80^{\circ}\text{C}$ .

#### **3.5.1.2. Determination of nucleic acid concentrations**

The concentration of the nucleic acid solutions was calculated using the NanoDrop<sup>®</sup> Spectrophotometer ND-1000 by determining the OD at 260 nm ( $\text{OD}_{260\text{ nm}}$ ). The ratio of  $\text{OD}_{260\text{ nm}}/\text{OD}_{280\text{ nm}}$  was used to determine the purity of the RNA solution, which should be  $\sim 2$ .

#### **3.5.1.3. Reverse transcription**

Reverse transcription was performed to generate complementary DNA (cDNA) from isolated RNA. Equal amounts of RNA (0.5 – 1.5  $\mu$ g) were diluted in autoclaved ddH<sub>2</sub>O, performing a 11  $\mu$ L solution, and heated to  $70^{\circ}\text{C}$  for 10 min to linearize the RNA. After short centrifugation and incubation on ice, 1  $\mu$ L of oligo(dT) primer, 4  $\mu$ L 5 x reaction buffer, 2  $\mu$ L dNTP mix (10 mM each), 1.5  $\mu$ L ddH<sub>2</sub>O and 0.5  $\mu$ L 200 U  $\mu\text{L}^{-1}$  RevertAid<sup>™</sup> Minus Reverse Transcriptase were added. After brief mixing, an incubation step was carried out at  $37^{\circ}\text{C}$  for 10 min to ensure effective annealing of the primer to the template, followed by the elongation step of the cDNA synthesis at  $42^{\circ}\text{C}$  for 1 h. After short centrifugation, the enzyme was heat-inactivated at  $70^{\circ}\text{C}$  for 10 min. Finally, the obtained cDNA was stored at  $-20^{\circ}\text{C}$ .

#### **3.5.1.4. Quantitative real-time PCR**

Expression levels of cellular, viral, or bacterial mRNAs were analyzed by quantitative real-time PCR (qRT-PCR). After synthesis of cDNA, through reverse transcription of the mRNAs using an oligo(dT) primer or a random hexamer primer, amplification was performed with primers listed in 2.8.1. The amplification of the product is made in 3 steps: First there is the DNA

denaturation step, which occurs at elevated temperature (95 °C). Secondly, the annealing, where primers bind to complementary sequences, is done at 50-60 °C and third, the final extension step is made at 70-72 °C, which is the optimal temperature to the activity of DNA polymerase. This method uses the ability of a fluorescent dye (e.g. SYBR Green III) to intercalate or bind to dsDNA, allowing that the amplification of the double stranded PCR product to be detected by fluorescence. This means that the detected fluorescence is directly proportional to the amount of the amplified product.

The qRT-PCR was performed in 96-well plates. Per well, 7.2 µL of diluted cDNA (0.5 µl cDNA + 6.7 µl ddH<sub>2</sub>O) was mixed with 4.8 µL of reaction mix (4 µL 2 x Brilliant III SYBR Green QPCR Master Mix, 2 µL ddH<sub>2</sub>O and 0.6 µL primer mix (10 µL of fwd + 10 µL of rev in 100 µL of ddH<sub>2</sub>O)). Reactions were performed in technical duplicates. The qRT-PCR was performed using the Roche Light Cycler 480 II. Measurement of the expression of glyceraldehyde 3-phosphate dehydrogenase (GAPDH) mRNA was used for normalization. Specificity of amplification was assessed by investigation of melting curves of amplified PCR products. Analysis was performed by the  $2^{-\Delta\Delta C_T}$  method (Livak and Schmittgen, 2001).

### **3.5.2. Proteins**

#### **3.5.2.1. Preparation of protein lysates**

To analyze protein expression after singular viral or bacterial as well as co-infection, the cell monolayer was washed with PBS and lysis was performed by adding 200 µL RIPA buffer supplemented with a protease inhibitor mix to each well, in 6-well plates. Cells were detached using a scraper. Cell lysates were then transferred into reaction tubes and centrifuged at 20187 rcf for 10 min at 4 °C. The supernatants were subsequently used to determine the protein concentration (see section 3.5.2.2). For long-term storage of the samples, they were kept at – 20 °C.

### **3.5.2.2. Determination of protein concentrations**

To normalize the protein levels for SDS-PAGE and Western Blots, relative protein concentration was determined by using the Bradford Assay. This assay, a colorimetric protein assay, is based on an absorbance shift of the dye Coomassie Brilliant Blue G-250. Binding to a protein results in a shift of the absorption maximum to 595 nm, which can be measured (Bradford, 1976). To determine the protein concentration, 5  $\mu$ L of the clear protein lysates were added to 1000  $\mu$ L 1  $\times$  Bradford reagent (Bio-Rad Protein Assay Dye Reagent; concentrate diluted in ddH<sub>2</sub>O) in a cuvette and mixed. Bradford Reagent served as blank sample. The absorption at 595 nm was measured with a spectrophotometer. Finally, the protein concentrations within one experiment were adjusted. The calculated amount of sample was mixed with RIPA buffer according to the individual protein concentration and 40  $\mu$ L of 5  $\times$  SDS-PAGE sample buffer was added to perform 200  $\mu$ L samples.

### **3.5.2.3. Discontinuous SDS polyacrylamide gel electrophoresis (SDS-PAGE)**

The electrophoretic separation of proteins was performed by discontinuous SDS polyacrylamide gel electrophoresis (SDS-PAGE). Via SDS-PAGE proteins are separated according to their molecular weight, based on their differential rates of migration through a matrix (a gel) under the influence of an applied electrical field. To achieve the separation of the proteins according to their molecular weight, the samples were boiled for 7 mins at 96 °C. The SDS and the  $\beta$ -2-mercaptoethanol in the SDS-PAGE buffer lead to the denaturation and linearization of the proteins. SDS binds to linearized proteins, thereby introducing a uniform negative charge. The  $\beta$ -2-mercaptoethanol is the reducing agent that breaks down protein-protein disulphide bonds. This way, proteins can migrate through the gel matrix according to their molecular weight. The separation was made on discontinuous gels consisting of a stacking gel and a running gel. Polyacrylamide is a matrix formed from monomers of acrylamide and bis-acrylamide. The polymerization reaction is initiated by

TEMED, which induces a free radical formation from ammonium persulfate (APS). The stacking gels present bigger pores due to a lower concentration of polyacrylamide). Due to the pH change from the stacking gel (pH 6.8) to the running gel (pH 8.9), proteins are stacked before the separation in the running gel, which contains small pores allowing the separation of proteins according to their molecular weight. For this, 20-30  $\mu\text{L}$  of each sample were applied to the polyacrylamide gel for separation. Electrophoresis was first run at 20 milliamps (mA) in a buffer filled chamber (1x SDS-PAGE buffer) until the protein bands reached the cut off gel border and then increased to 40 mA. For comparison, 5  $\mu\text{L}$  of the size standard PageRuler™ were used, whose band pattern resulted in a subsequent size allocation of the proteins.

#### **3.5.2.4. Western Blot and immunodetection**

For visualization, proteins separated by SDS-PAGE were transferred to a nitrocellulose membrane by western blotting (WB). A gel-membrane-filter sandwich is placed in a blotting chamber, suspending in blotting buffer vertically. Proteins transfer from the gel to the membrane under the control of a constant 400 mA electric field produced by electrode plate parallel to the sandwich for 55 min.

For detection of proteins, the nitrocellulose membranes were incubated on blocking solution for 1 h, shaking and at room temperature (RT). Incubation with diluted primary antibody (in TBST + 5 % BSA) was done overnight at 4 °C. Then, the antibody solution was removed, the membranes were washed with TBST buffer three times for 5 min before the HRP conjugated secondary antibodies, also diluted in TBST, were added for 1 h, shaking at RT. Then, the membrane was once again washed three times for 10 min with TBST, before ECL was added for 1 min at RT. The HRP catalyzes the oxidation of luminol, which leads to emission of light that was detected by digital imaging with a CCD camera system. Another alternative was to add IRDye® conjugated secondary antibodies, instead of HRP conjugated ones, which allowed detection of two targets simultaneously. In this case, the ECL solution is not

needed, since the fluorophores re-emit fluorescent signal upon light excitation. This signal was detected with the same instrument.

#### **3.5.2.5. Determination of cytotoxicity by activity measurement of Lactate dehydrogenase (LDH)**

LDH is an exclusively intracellular enzyme that plays a key role in lactic acid fermentation and catalyzes the formation of lactate and NAD<sup>+</sup> from pyruvate and NADH. When the membrane of a cell is damaged, LDH is released into the extracellular space along with many other cellular components. To determine cytotoxicity, the supernatants of singular or co-infected A549 cells were analyzed using an LDH-mediated color reaction and the CytoSelect™ LDH Cytotoxicity Assay Kit (Cell Biolabs), where the rate of cytotoxicity is directly proportional to the intensity of the color reaction. For this purpose, cells were seeded in duplicates and infected as described before. At the end of the experiment, the 90 µL of the supernatant was transferred to a 96-well plate with a flat bottom and mixed with 10 µL each of the LDH cytotoxicity assay reagent. The plate was incubated for 30 min at 37 °C and the intensity of the color reaction determined by measuring the OD<sub>450 nm</sub> on the SpectraMax M2.

#### **3.5.2.6. Detection of secreted cytokines and chemokines via Fluorescence-activated cell sorting (FACS)**

Flow cytometric analysis allows characterization of cells, but also quantification of the absolute amount of secreted cytokines and chemokines in a solution. For this purpose, Biolegend's bead-based immunoassay LEGENDplex™ was used. With this kit, up to 13 cytokines can be detected in one sample at the same time. The beads are each coupled with the cytokine-specific antibodies and can be distinguished by their size in two different populations. Each population in turn can be differentiated from each other by their reference fluorophore allophycocyanin. When a selected panel of capture beads are mixed together and incubated with an unknown sample containing target analytes, each analyte will be bound by its specific capture bead. By

subsequent incubation with streptavidin-phycoerythrin (SA-PE)-coupled secondary antibodies the amount of each cytokine can be individually determined cytometrically using a calibration line (Probst *et al*, 2003). For the analysis of secreted cytokines, 6  $\mu$ L of the respective supernatant of infected cells or of the calibration standard were used in a ratio of 1: 3 with 18  $\mu$ L of the reaction solution consisting of 6  $\mu$ L assay buffer, 6  $\mu$ L beads and 6  $\mu$ L detection antibody in 96-well plates. The samples were then incubated shaking for 2 h (600 rpm) at RT protected from light. After the incubation period, in each case 6  $\mu$ L of SA-PE conjugate were added per sample and incubated shaking for further 30 min. The beads were then pelleted at 1000 x g for 5 min, the supernatant discarded, and the beads resuspended in 150  $\mu$ L of the wash buffer contained in the kit and recentrifuged. For quantification of the cytokines, the samples were upmixed in 150  $\mu$ L wash buffer and analyzed on the FACSCalibur™ flow cytometer (BD) according to the manufacturer's instructions. The quantitative evaluation was carried out using the LEGENDplex™ software.

## 4. Results

### 4.1. Bacterial and viral co-infection increases the cell damage and death

*S. aureus* is able to colonize individuals without causing any symptoms. But it is known that superinfections with *S. aureus* often results in excessive inflammation and tissue damage (Chertow and Memoli, 2013; Löffler *et al.*, 2013). Thus, investigation of a primary bacterial exposure and its effects on a consequent viral infection is as important as primary viral and subsequent IAV infection. Interestingly, in tissue cultures this damaging effect is also observed and leads to a strong decrease in overall cell viability. Within the present study, different infections times, multiplicities of infection (MOIs) and infection orders were tested. The bacterial infection was done prior to the viral infection and two infection settings were performed (Fig. 1). During the first part of the study cell viability was in focus of interest. Within the first scenario cells were infected for 32 h starting with bacterial infection at a MOI of 0.001 for 24 h. Subsequently viral infection was performed at a MOI of 1 for 8 h. Within the second scenario infection was performed for 48 h, again starting with a bacterial infection as already described. The difference concerned the viral infection. Instead of 8 h, the viral infection was performed with two different MOIs, 0.1 or 0.5, and for 24 h.

A549 cells were infected with *S. aureus* 6850 wt and with PR8M as described above and visually evaluated by light microscopy. Cytotoxicity was measured by LDH release (Fig. 2).

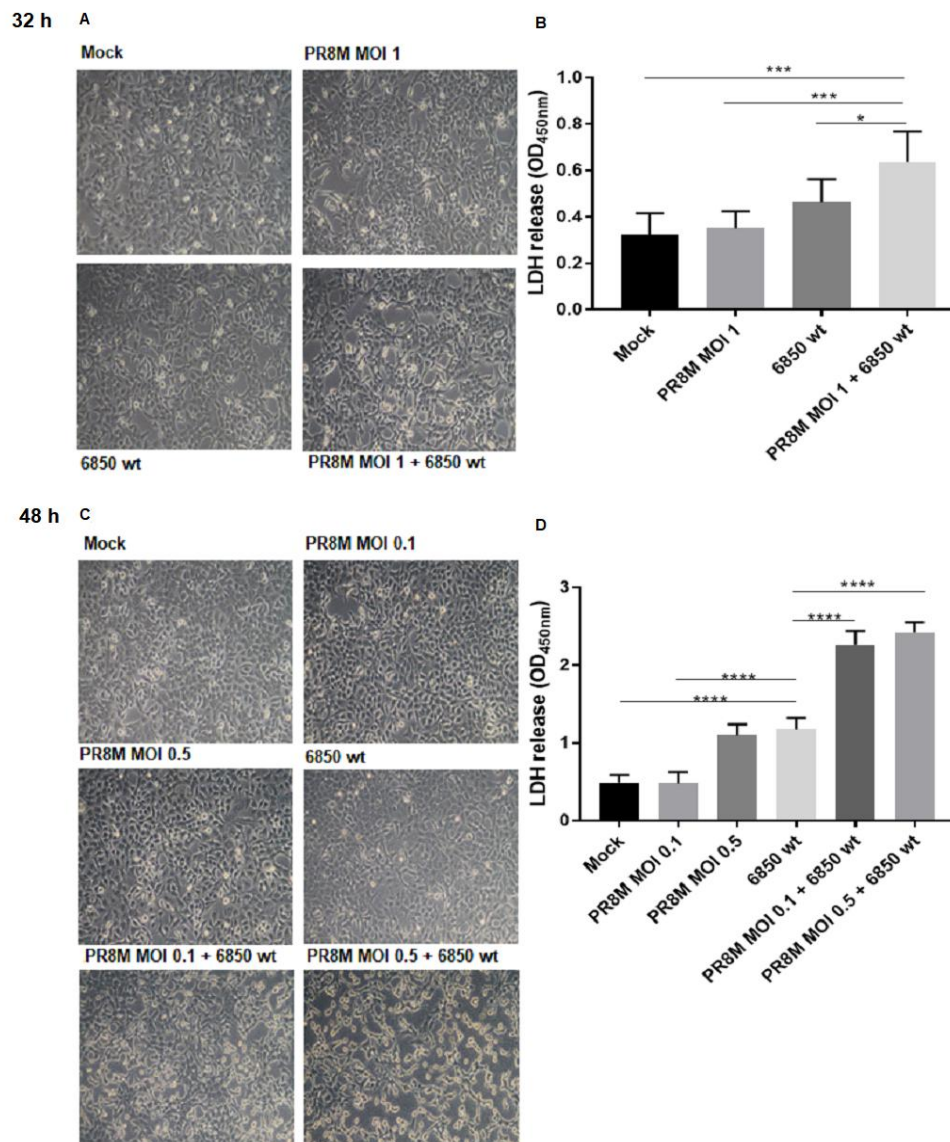


**Figure 6 - Cell damage is increased in co-infected cells.** A549 cells were infected with *S. aureus* 6850 wt (MOI 0.001) for 3 h. This was followed by a 20 min wash step with lysostaphin to remove any non-internalized bacteria. An additional 30 min wash step with gentamicin was performed at 6 h p.i. At 24 h post bacterial infection cells were co-infected with influenza A/Puerto Rico/8/34 (PR8M) (MOI 1) (A, B) or (MOI 0.1 or 0.5) (C, D) for 30 min. (A, B) At 32 h p.i. cells were monitored by light microscopy and the supernatants were taken to perform an LDH cytotoxicity assay. (C, D) Additionally, at 32 h p.i. a 30 min wash step with gentamicin was performed. At 48 h p.i. cells were observed at light microscopy and pictures were taken (C). Supernatants were removed to perform an LDH cytotoxicity assay (D). The intensity of the assay color reaction was determined by measurement of the OD<sub>450 nm</sub> (B, D). Results show representative pictures of one experiment (A, C) and the mean values + standard deviation

(SD) of three independent experiments (B, D). Statistical significances were determined by one-way ANOVA followed by Tukey's (B) and Dunnett's (D) multiple comparison test (\*\*\*\*  $p \leq 0.0001$ ; \*\*\*  $p \leq 0.001$ ; \*  $p \leq 0.1$ ).

Cell pictures show that in both experimental settings infection results in cytopathic effects (CPE) although to different extents. At 32 h p.i. CPE effects aren't strong, and the cell monolayer is still intact. However, slight differences are visible, when comparing mock-treated, single and co-infection scenarios (Fig. 2 A). While mock-treated cells are completely intact, CPE increases from singular IAV or *S. aureus* and to co-infection. These results nicely correlate to the LDH cytotoxicity assay (Fig. 2 B). Similar is true for the 48 h infection scenario. During infection times of about 48 h, the CPEs get much stronger and the differences between the various scenarios are higher (Fig. 2 C). While morphology of cells, infected with 0.1 MOI IAV is comparable to that of mock treated cells, CPE increases with the viral burden. The bacterial infection induced damage is more pronounced than in mock and IAV (MOI 0.1) infected cells, however like that of cells infected with 0.5 MOI IAV. Thus, the CPE correlates to initial infection doses and times of infection. Again, the enhanced CPE is accompanied by higher LDH release (Fig. 2 D).

In summary both experimental settings (32 h and 48 h) result in cell damage and destruction depending on infectious doses and times of infection (Fig. 2 A and C). Furthermore, the destruction can be determined by measurement of LDH release, which reflects changes in cell morphology (Fig. 2 B and D).

#### **4.2. Pathogen load is enhanced upon co-infection**

The first experimental settings indicate that the cell damage and cell death are increased upon co-infection. The next step was to determine if this increased destruction could be related to an increase in pathogen load during the infection. Former studies have shown that combined IAV and *S. aureus* infection results in increased pathogen load, tissue damage and changes in immune response (Iverson *et al.*, 2011). A549 cells were infected under the same conditions as described in section 4.1. Subsequently, supernatants were

used to determine progeny viral particles by standard plaque assay on MDCKII cells as well as extracellular bacterial titers by serial dilution on agar plates. Additionally, intracellular bacterial titers were determined upon cell lysis (Fig. 3).

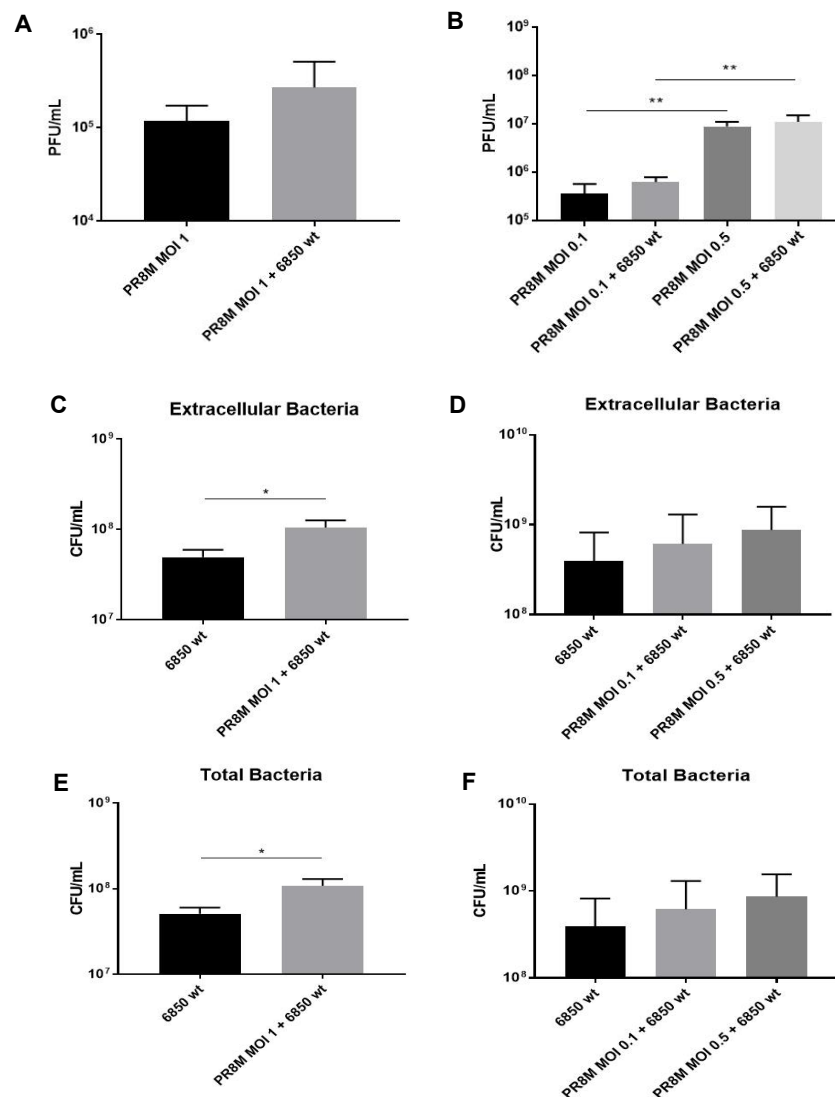


**Figure 7 - Viral and bacterial titers are enhanced upon co-infection.** A549 cells were incubated with *S. aureus* 6850 wt (MOI 0.001) for 3 h. This was followed by a wash step with lysostaphin for 20 min to remove any non-internalized bacteria. An additional wash step with

gentamicin for 30 min was performed at 6 h p.i. 24 h p.i. cells were infected with PR8M (A, C, E) (MOI 1) or (B, D, F) (MOI 0.1 or 0.5) for 30 min. At 32 h p.i. supernatants were removed, and viral (A) and bacterial titers were determined (C and E). For longer infection periods (B, D, F) an additional wash step was performed at 32 h p.i. for 30 min with gentamicin. At 48 h p.i. supernatants were removed, and viral (B) and bacterial (D, F) titers were analyzed. Furthermore, cells were lysed for investigation of intracellular bacterial titers. Viral titers (A, B) were determined by standard plaque-assay while extracellular and intracellular bacterial titers (C, D) were determined by serial dilution and plating on BHI-medium agar plates. For extracellular titers the supernatants were taken, and for intracellular titers cells were lysed by osmotic shock, and the lysates were then used. From these experiments, total bacterial titers (E, F) were obtained by adding the values of extracellular and intracellular bacterial titers from each experiment. Results show the mean values + SD of three independent experiments. Statistical significances were determined by unpaired t-test with Welch's correction (A, C, E) and by one-way ANOVA followed by Tukey's (B, D, F) multiple comparison test (\*  $p \leq 0.1$ ; \*\*  $p \leq 0.01$ ).

Investigation of the viral load at 32 h p.i. (Fig. 3 A) indicates enhanced replication in presence of both pathogens in comparison to singular infection (Fig. 3 A). At later times of infection (Fig. 3 B) significant enhancement of the pathogen burden is not visible. Thus, enhanced viral titers depend on the initial MOI used. Comparing both graphs (Fig. 3 A and B), it becomes obvious that the viral loads reach higher values within 48 h of infection, although lower infection doses were initially used.

Regarding the bacterial load, data indicate an increase of extracellular and intracellular bacterial titers 32 h upon co-infection (Fig. 3 C and E). At 48 h upon co-infection (Fig. 3 D and F), enhancement of bacterial titers is not significant but an increasing tendency is still detected. Correlating to viral titers (Fig. 3 A and B), bacterial load increases during ongoing infection. Intracellular bacteria titers were also analyzed. Since the intracellular bacterial amounts are substantial lower than the extracellular bacterial titers, which is also reflected by the total bacterial amount, data are not depicted.

In summary, the pathogen burden, either bacterial or viral, reach higher values during ongoing infection. While a tendency of increased viral titers is observed (Fig. 3 A), significant enhancement of bacterial titers is visible upon 32 h (Fig. 3 C and E) in presence of both pathogens in comparison to singular

infection. At 48 h p.i. the viral load increases independent on the MOIs used for infection (Fig. 3 B) and the bacterial titers are enhanced as well (Fig. 3 D and F).

To gather more information on how the viral and bacterial load is correlated to the increase of destruction and damage observed during co-infection, viral and bacterial mRNA synthesis as well as the protein expression had to be determined. For this reason, qRT-PCR and Western Blot analysis were performed. The viral M1 mRNA, the viral PB1 protein expression and bacterial PGN protein synthesis were monitored (Fig 4). Interestingly, data are in line with the pathogen titers.

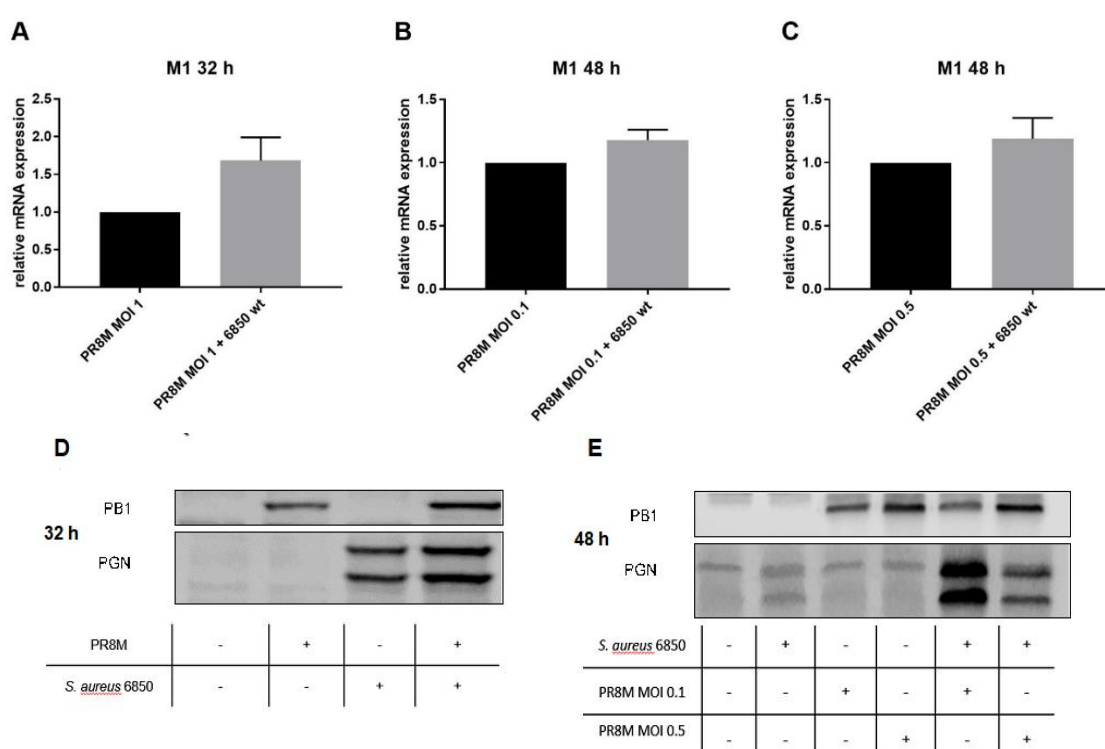


**Figure 8 - Upon co-infection mRNA and protein synthesis of both pathogens is increased. A549 cells were incubated with *S. aureus* 6850 wt (MOI 0.001) for 3 h. This was followed by a 20 min wash step with lysostaphin to remove any non-internalized bacteria. An additional 30 min wash step with gentamicin was performed at 6 h p.i. At 24 h p.i. cells were infected with PR8M (MOI 1) (A, D) or (MOI 0.1 or 0.5) (B, C, E) for 30 min. At 32 h p.i. cells were lysed, RNA extracted and isolated, cDNA synthesized, and qRT-PCR was performed (A)**

or the cells were lysed, protein lysates were obtained and SDS-PAGE and Western Blots were performed, proteins were then immunodetected (D). For longer times of infection (B, C, E), at 32 h p.i. an additional 30 min wash step with gentamicin was performed. At 48 h p.i. cells were lysed, RNA extracted and isolated, cDNA synthesized, and qRT-PCR was performed (B, C) or the cells were lysed, protein lysates were obtained, and SDS-PAGE and Western Blots were performed (F). The viral PB1 and the bacterial PGN proteins were detected using specific antibodies. Results show the mean values + SD of three independent experiments (A, B, C) or representative data from three experiments (D, E). Statistical significances were determined by unpaired t-test with Welch's correction (A, B, C).

At 32 h upon infection, increased viral M1 mRNA synthesis (Fig. 4 A), PB1 protein expression (Fig. 4 D) as well as bacterial PGN protein expression are observed in presence of both pathogens. However, 48 h upon infection enhancement of mRNA synthesis and protein expression is not significant (Fig. 4 B, C and E), which nicely correlates with the results of viral titers shown in Fig. 3. Bacterial mRNA levels were also investigated, but due to technical difficulties the results are not shown. Nevertheless, PGN levels also nicely correlate with the bacterial titers, except at 48 h p.i.. At 32 h and 48 h upon co-infection increased PGN expression is detected in comparison to singular bacterial infection (Fig. 4 D, E). However, enhanced bacterial protein expression, decline with higher viral infectious doses at 48 h p.i..

In summary, the data indicate an increased tendency of the viral and the bacterial loads upon co-infection. These data are verified by the viral and bacterial titers, by M1 synthesis (viral protein), as well as PB1 and PGN expression.

### **4.3. Immune response**

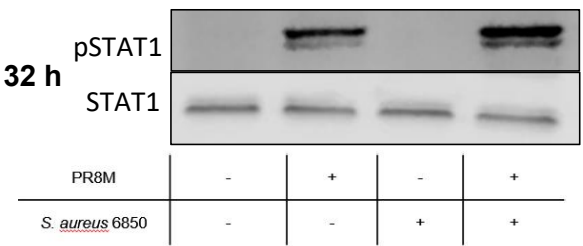
The co-pathogenesis of combined IAV and *S. aureus* infections might be explained by several factors. Compromised immune functions, up-regulation of viral entry receptors, synergistic effects on inflammation and tissue damage, but also changes in the innate immune response might explain the patient susceptibility to both pathogens (Iverson *et al.*, 2011; Bellinghausen, 2016). So far, we observed an increase of the cell damage and death, as well an increasing tendency of the pathogen burden during co-infection. In a next step

regulation of cellular mechanisms in response to IAV and *S. aureus* co-infection were examined. For this reason, immune responses were monitored on the level of mRNA synthesis and protein expression of several immune regulatory factors upon viral and bacterial infection.

A549 cell were infected for 32 h and 48 h as described above.

### 4.3.1. Induction of type I IFN- $\beta$ and downstream factors is enhanced in

**A**



presence of IAV and *S. aureus*

**B**

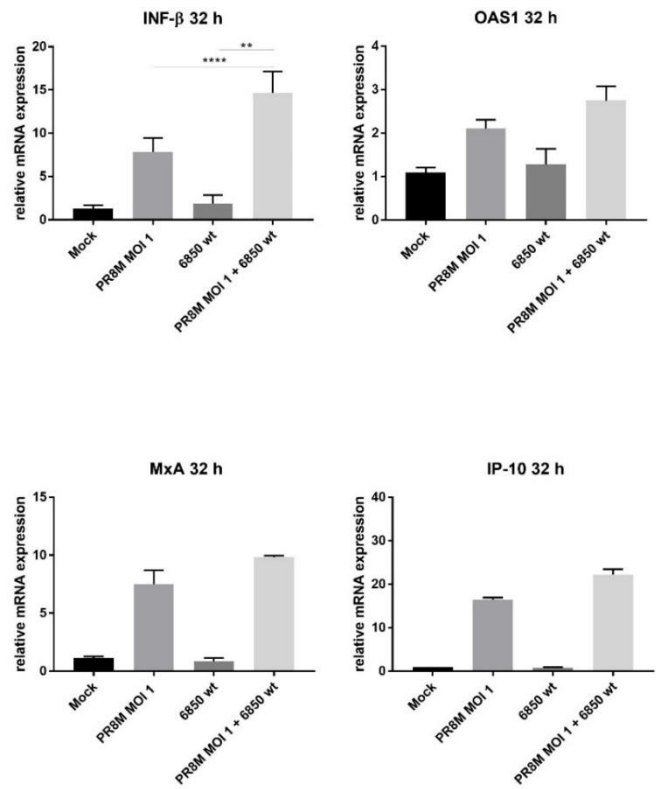


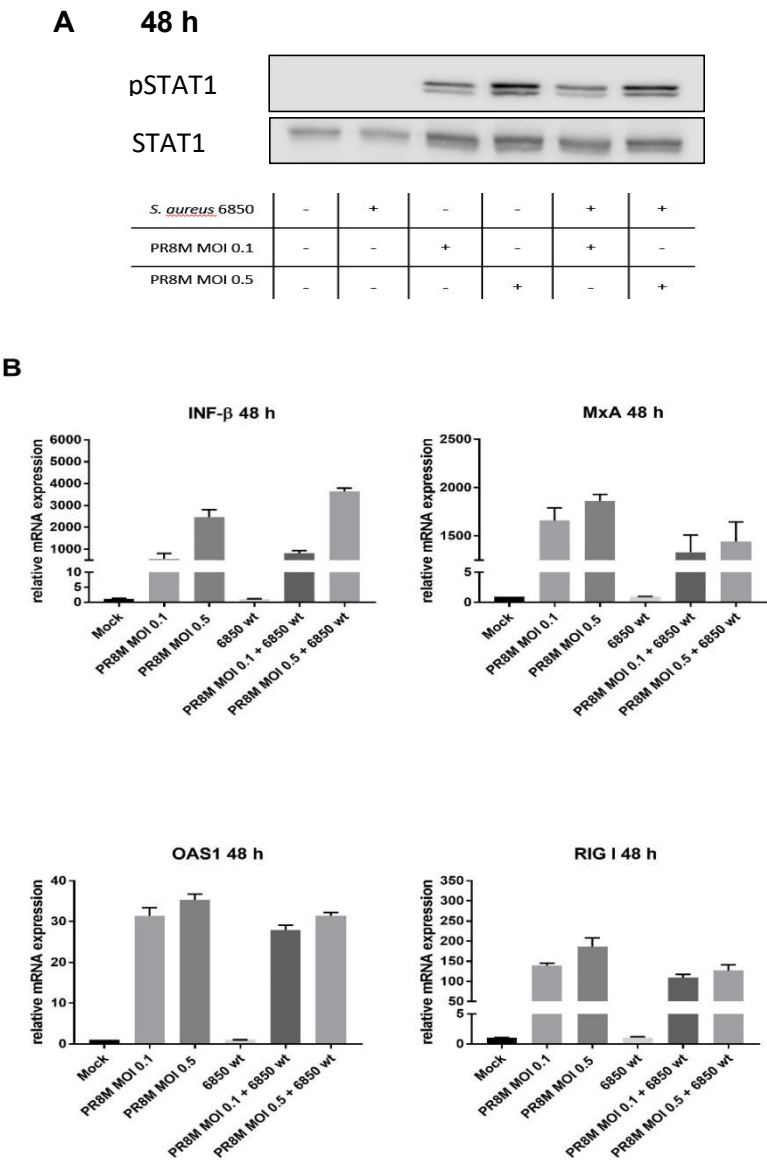
**Figure 9 - Expression of type IFN- $\beta$  and ISGs is enhanced upon viral and bacterial co-infection.** A549 cells were infected with *S. aureus* 6850 wt (MOI 0.001) for 3 h. This was followed by a 20 min wash step with lysostaphin to remove any non-internalized bacteria. An additional 30 min wash step with gentamicin was performed at 6 h p.i. At 24 h p.i. cells were infected with PR8M (MOI 1) for 30 min. At 32 h p.i. cells were lysed, protein lysates were performed and subjected to Western Blot analysis (A). Alternatively, RNA was isolated and subjected to qRT-PCR (B). The experiments were performed three times and one representative Western Blot analysis (A) or the mean values + SD of: IFN- $\beta$  (3 independent experiments (3x)); MxA (2x); 2'-5'-oligoadenylate synthetase 1 (OAS1) (2x); IP-10 (2x) are shown. Statistical significances for IFN- $\beta$  results were determined by one-way ANOVA followed by Tukey's multiple comparison test (\*\*  $p \leq 0.01$ ; \*\*\*\*  $p \leq 0.0001$ ).

Western Blot analysis shows slightly increased phosphorylation of STAT1 (pSTAT1) 32 h upon co-infection in comparison to single viral infection. STAT1 is not phosphorylated in control or *S. aureus* infected samples (Fig. 5 A). Concomitantly, the mRNA expression of other cellular factors, either involved in STAT1 regulation or regulated by STAT1, is enhanced (Fig. 5 B). Exemplarily, IFN- $\beta$  that represents an upstream intervenient of this pathway was investigated. Interaction of IFN- $\beta$  with IFNAR results in induction of the JAK-STAT signaling pathway (Ehrhardt, 2010). The mRNA synthesis of IFN- $\beta$  increases from single viral to co-infected cells, while no expression is observed in control and bacterial infected cells. Similarly, the mRNA synthesis of ISGs, such as OAS1 and MxA is increased upon combined, comparing to single viral infection, although, the overall expression levels aren't high. Once again, in *S. aureus* infected and control cells the expression of these ISG is not visible comparing to viral and co-infected samples.

Interestingly, the examination of different cytokines and chemokines showed an increase in IP-10 mRNA synthesis in presence of IAV and *S.*

*aureus* in comparison to single viral infection, while control and single *S. aureus* infected cells, don't show relevant expression.

### 4.3.2. Phosphorylation of STAT1 and mRNA synthesis of downstream elements are reduced upon co-infection



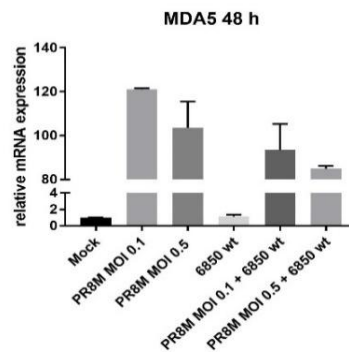


**Figure 10 - Phosphorylation of STAT1 and mRNA synthesis of downstream factors are reduced upon co-infection.** A549 cells were infected with *S. aureus* 6850 wt (MOI 0.001) for 3 h. This was followed by a 20 min wash step with lysostaphin to remove any non-internalized bacteria. An additional 30 min wash step with gentamicin was performed at 6 h p.i.. At 24 h p.i cells were infected with PR8M (MOI 0.1 or 0.5) for 30 min. At 32 h p.i. a 30 min wash step with gentamicin was performed. At 48 h p.i. cells were lysed and (A) proteins were examined by Western Blot analysis or (B) RNA was extracted, cDNA synthesized, and mRNA synthesis was analyzed by qRT-PCR. All the experiments were performed three times. (A) Results are representative data from three experiments or (B) show the mean values + SD of: IFN- $\beta$  (2x); MxA (2x); OAS1 (2x); RIG-I (1x); MDA5 (2x).

During longer times of infection, phosphorylation of STAT1 is increased correlating to rising viral infectious doses. Interestingly, upon combined viral and bacterial infection a reduction of pSTAT1 is observable. Once again, control and bacterial infected cells don't show an expression of the phosphorylated protein levels (Fig. 6 A).

In line with these results, qRT-PCR analyses indicate higher mRNA expression levels than observed 32 h p.i. (Fig. 6 B). Furthermore, IFN- $\beta$  mRNA expression is increased in co-infected in comparison to PR8M infected cells, while in control- and *S. aureus* infected cells IFN- $\beta$  mRNA expression is not detectable. With increasing viral infection doses enhanced IFN- $\beta$  expression is detected. However, investigation of downstream factors of the JAK-STAT mediated signaling pathway, such as MxA, MDA5 and OAS1 shows a declining tendency from single viral to co-infected samples, nicely correlating with the reduction on pSTAT1 seen in Western Blot analysis (Fig. 6A). Once again, in

control and bacteria infected cells mRNA synthesis of ISGs is not detectable. Nonetheless, MxA and OAS1 mRNA synthesis correlates to the viral infectious dose used. In presence of both pathogens MDA5 mRNA levels show a reduction.

Retinoic acid inducible gene I (RIG-I) is a pattern recognition receptor that induces IFN expression (Hiscott, 2006). We were not able to detect RIG-I mRNA synthesis in control and bacterial infected cells. However, virus induced RIG-I mRNA synthesis is increased with rising infection doses and reduced in presence of IAV and *S. aureus*.

### 4.3.3. Cytokine and chemokine expression are increased during co-infection

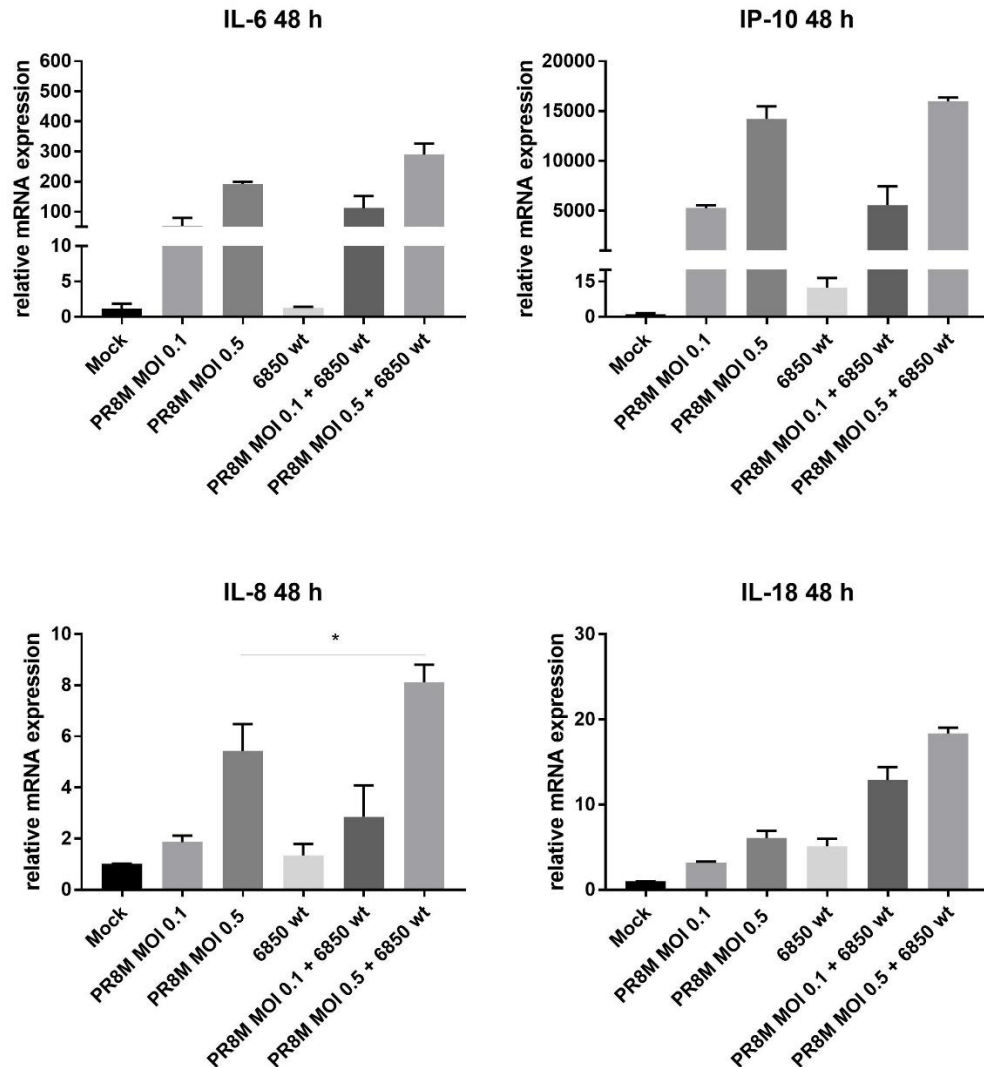


**Figure 11 - Cytokine and chemokine expression is increased upon co-infection.** A549 cells were infected with *S. aureus* 6850 wt (MOI 0.001) for 3 h. This was followed by a 20 min wash step with lysostaphin to remove any non-internalized bacteria. An additional 30 min wash step with gentamicin was performed at 6 h p.i.. At 24 h p.i cells were infected with PR8M (MOI 0.1 or 0.5) for 30 min. At 32 h p.i. a 30 min wash step with gentamicin was performed. At 48 h p.i. cells were lysed and (A) proteins were examined by Western Blot analysis or (B) RNA was extracted, cDNA synthesized, and mRNA synthesis was analyzed by qRT-PCR. All the experiments were performed three times. (A) Results are representative data from three experiments or (B) show the mean values: IP-10 (2x); IL-6 (1x); IL-8 (3x) and IL-18 (1x).

Statistical significances for IL-8 results were determined by one-way ANOVA followed by Tukey's multiple comparison test (\*  $p \leq 0.1$ ).

Synthesis of cytokines and chemokines is induced upon PR8M infection and increased with rising infectious doses (Fig. 7). While single viral infection results in induction of IL-6, IL-8, IL-18 and IP-10 mRNA synthesis, single bacterial infection stimulates only IL-8, IL-18 and IP-10 mRNA synthesis. In presence of *S. aureus* the IAV induced IL-6, IL-8 and IL-18 mRNA expression is enhanced 48 h p.i..

#### **4.3.4. IL-18 secretion is increased during co-infection**

It is known that pulmonary pathologies are caused, among others, by IL-1 $\beta$  and the IL-18 cytokines. Both are major components of the inflammasome, which is activated by *S. aureus* (Parker and Prince, 2012). At the same time, due to the activation of the inflammasome, pyroptosis, a highly inflammatory form of cell death is induced (Munoz-Planillo, 2009; Lappalainen and Whitsett, 2005).

Since IL-18 mRNA synthesis was enhanced upon co-infection, IL-18 protein secretion was monitored (Fig. 8). To prevent the elimination of secreted proteins, instead of a washing step at 32 h p.i., the supernatants were transferred to Eppendorf reaction tubes and centrifuged at 20817 rcf for 2 min. Hereby, extracellular bacteria were removed without extracting virus particles, secreted cytokines and chemokines. Afterwards, the supernatant was transferred back to the corresponding wells until the end of the experiment.

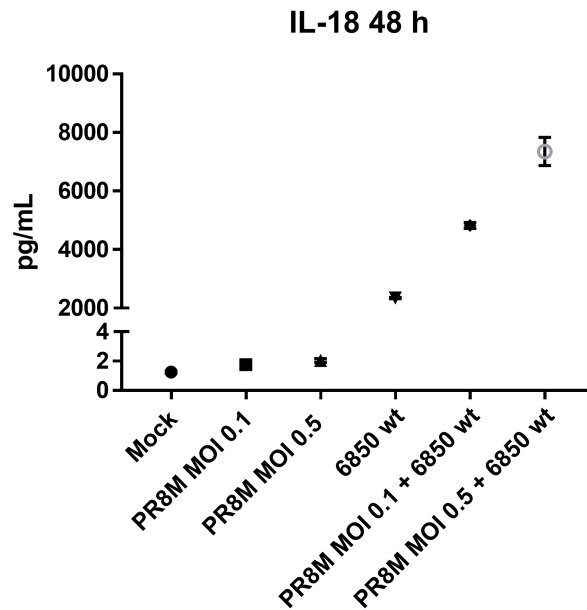


**Figure 12 - The IL-18 protein synthesis and secretion is increased upon co-infection.**

A549 cells were infected with *S. aureus* 6850 wt (MOI 0.001) for 3 h. This was followed by a 20 min wash step with lysostaphin to remove any non-internalized bacteria. An additional 30 min wash step with gentamicin was performed at 6 h p.i.. At 24 h p.i cells were infected with PR8M (MOI 0.1 or 0.5) for 30 min. At 32 h p.i. supernatants were transferred to Eppendorf reaction tubes, centrifuged at 20817 rcf for 2 min. Afterwards, the medium was transferred back to the corresponding wells until the end of the experiment. At 48 h p.i. supernatants were collected. For quantification of the cytokines the FACSCalibur™ flow cytometer was used. This experiment was performed two times.

Low levels of IL-18 secretion are detected in control and viral infected cells, whereas increased levels are observed upon *S. aureus* infection. Comparison of single bacterial infection to co-infected samples indicates an increased amount of the IL-18 secretion, correlating with the viral infectious dose, which was used in the co-infection.

## 5. Discussion

Influenza infections are a major concern in public health and, worse, when they suffer complications due to other factors such as secondary or concomitant bacterial infections. During the Spanish flu 50 million people died, being this great part due to bacterial co-infections (Taubenberger and Morens, 2006). Recently *S. aureus* has become important due to the appearance of more resistant strains (Wertheim *et al.*, 2005) and due to the increase of cases of co-infections caused by this bacterium. Therefore, it is important to know the development of this disease, under the influence of other pathogens, to help understand the mechanisms of development of this type of co-infection, to estimate the pathogenicity and to create new therapies to combat this type of disease.

The main goal was then to observe if the primary bacterial exposure would prime the cells to a subsequent viral infection or if the development of tolerance or resistance would take place.

### 5.1. Cell damage is increased upon co-infection

Influenza and bacterial co-infection results in significant morbidity and mortality (Chertow and Memoli, 2013). Former studies have shown that combined IAV and *S. aureus* infections lead to increased pathogen load, tissue damage and changes in immune responses (Iverson *et al.*, 2011). Further, IV and bacteria lethal synergy has been demonstrated in animal models, and it is known that IV infections contribute to epithelial cell dysfunction and death by disrupting protein synthesis and induction of apoptosis (Perales *et al.*, 1995; Mori *et al.*, 1995; Hinshaw *et al.*, 1994). The viral NA cleaves sialic acids, also of respiratory epithelial cells, and was shown contribute to increased bacterial adhesion and dissemination (Peltola *et al.*, 2005; McCullers, 2004). Sloughed host cells and increased mucus production in the airways are a source of nutrient for bacteria growth (Siegel *et al.*, 2014). In the other hand, protease

activity by *S. aureus* was introduced to increase IAV virulence by cleaving HA (Tashiro *et al.*, 1987; Tashiro *et al.*, 1987).

In the present study we were able to show that infection with IAV and/or *S. aureus* results in CPE to different extents. Upon co-infection, the damage of the cell monolayer is higher, comparing to single infections, but also longer infection times contribute to cell damage and destruction, correlating to the increased pathogen load (Fig. 3 and 4).

## **5.2. Cytokine and chemokine are enhanced during viral and bacterial co-infection**

Interestingly, our data indicate an enhanced expression of IL-6, IL-8, IL-18 and IP-10 cytokines and chemokines in presence of IAV and *S. aureus* infection concomitant to induction of tissue damage.

Enhanced pathogenesis during co-infection is a result of complex interactions among immune cells, which evoke synergistic inflammatory responses and disrupt the integrity of the epithelial barrier. Several factors and mechanisms contribute to a so called “cytokine storm” during infection with different pathogens (Conenello *et al.*, 2007). Cytokines belong to large families of soluble molecules with pro- or anti-inflammatory properties. In the lungs a cytokine storm can lead to irreparable tissue destruction. Pro-inflammatory cytokines, such as IL-6 and IL-8 are required for immune protection, but in case of overproduction become toxic.

Another cytokine that can be involved in lung pathology is IL-18, which is a major component of the inflammasome and is activated by *S. aureus* (Parker and Prince, 2012; McGilligan *et al.*, 2013; Melehani and Duncan, 2016). Interestingly IL-18 was shown to induce pyroptosis, a highly inflammatory form of cell death (Bergsbaken, 2009; Munoz-Planillo, 2009; Lappalainen and Whitsett, 2005).

Thus, these observations are in line with our results showing enhanced levels of IL-6, IL-8, IL-18 and IP-10 cytokines and chemokine synthesis in presence of IAV and *S. aureus*. Notably, cell destruction and damage can be

linked to a “cytokine storm” caused by exacerbated and dysregulated immune response, especially in case of the high amounts of IL-18 cytokine secretion.

### **5.3. Blockade of anti-viral response**

In response to viral and bacterial co-infection, a complex interaction of cellular mechanisms is initiated, that is responsible for regulating the immune response against pathogens. However, at the same time, pathogen supportive functions are induced, as well. Upon combined IV and *S. aureus* infections higher pathogen load, changes in immune response and tissue damage are known to occur (Iverson, 2011).

In the first line of defence against viral pathogens, is the type I IFN response, which was also shown to fulfil anti-bacterial functions (Randall and Goodbourn, 2008; Parker and Prince, 2011). *In vivo* experiments verified that co-infections lead to higher levels of type I IFN expression (Kudva *et al.*, 2011; Parker and Prince, 2011).

As seen in section 1.2, the type I IFN response starts when IFN- $\beta$  interacts with IFNAR, activating the JAK-STAT pathway. Subsequently, STAT1 and STAT2 bind to IRF9 and form ISGF3 that leads to the transcription of several ISGs, such as the *Mx-1* and *Lif* (Martin FJ, *et al.*, 2009).

Remarkably, in an *in vitro* study it has been shown that metabolically active intracellular *S. aureus* inhibits type I IFN-mediated STAT1 phosphorylation and, consequently, STAT1-STAT2 dimerization, dampening the first line of defense against IV infection, which could lead to a more severe disease in a co-infection scenario (Warnking, 2015).

However, the two experimental *in vitro* settings that were performed within the present study showed different results, depending on time. Western Blot analysis performed at 32 hr upon infection indicated slightly increased phosphorylation of STAT1 (pSTAT1) and higher mRNA expression of other cellular factors, either involved in STAT1 regulation, such as IFN- $\beta$  or regulated by STAT1, like OAS1 and MxA. These results are in line with the common knowledge of JAK-STAT mediated signaling upon infection. However, at 48 hr after infection Western Blot analysis pointed to a reduction of pSTAT1

phosphorylation in presence of both pathogens. Furthermore, IFN- $\beta$  mRNA expression was increased in co-infected cells, while downstream factors of the JAK-STAT mediated signaling pathway, such as MxA, MDA5 and OAS1 shows a declining tendency from single viral to co-infected samples, nicely correlating with the reduced STAT1 phosphorylation. These results correlate to the results showed by Warnking and colleagues (Warnking, 2015), indicating the *S. aureus*-mediated interference with this pathway.

Interestingly, mRNA synthesis of RIG-I, which is a pattern recognition receptor of IAV that activates IFN expression (Hiscott, 2006), but itself is induced by type I IFN-mediated signaling and represents an ISG, is increased with rising infection doses and reduced in presence of IAV and *S. aureus*.

Thus, we were able to demonstrate that with longer infection periods, the block of the STAT1-STAT2 dimerization, by the bacteria happens, as showed by Warnking and colleagues (Warnking, 2015), which was not observed at shorter times of infection. Nevertheless, these discrepancies might be explained by changes in experimental settings, such as sequence of infection, initial infectious doses as well as times of infection. Rather, our results point to the necessity of high levels of internalized metabolic active *S. aureus* for interference with IAV-induced cellular mechanisms verifying the complex interplay of IV, *S. aureus* and their host in a pathogen load and time-dependent manner.

## 6. Conclusion

The results shown in this project support the hypothesis that prior exposure to bacteria can prime the cells for a secondary viral infection, since it is shown that upon combined infection the cell damage and destruction is higher. In correlation the pathogens load is increased, the immune response is exacerbated but the type I IFN response is impaired. However, these studies were performed *in vitro* with a single cell type and it's known that the immune response is the result of complex network interplay, between many types of cells, molecules and substrates. For this reason, more sophisticated model systems should be used, including at least different types of cells or cell cultures that could mimic the human lung environment but also *in vivo* models.

One of the main objectives of this project, was to adapt an experimental setting that could mimic a scenario, where a first bacterial exposure would happen prior to a viral infection, and that was fully accomplished. We determined infectious doses and times as well as read out systems, such as cell damage and cytokine expressions correlating to *in vivo* studies. The described experimental settings allow cheap and easy investigation to gain first insights in specific questions *in vitro*, which afterwards can be verified by complex ones.

## 7. References

1. Taubenberger, J. K. & Morens, D. M. The pathology of influenza virus infections. *Annu. Rev. Pathol.* 3, 499–522 (2008).
2. Taubenberger, J. K. & Kash, J. C. Influenza virus evolution, host adaptation, and pandemic formation. *Cell Host Microbe* 7, 440–51 (2010).
3. Hause, B. M. *et al.* Characterization of a novel influenza virus in cattle and swine: Proposal for a new genus in the *Orthomyxoviridae* family. *MBio* (2014).
4. Lamb, R., Krug, R. & Knipe, D. *Orthomyxoviridae: the viruses and their replication. Fields Virology* (2001).
5. Noda, T. Native morphology of influenza virions. *Front. Microbiol.* 2, 269 (2012).
6. Tong, S. *et al.* New world bats harbor diverse influenza A viruses. *PLoS Pathog.* 9, e1003657 (2013).
7. Bouvier, N. M. & Palese, P. The biology of influenza viruses. *Vaccine* 26 Suppl 4, D49–53 (2008).
8. Cheung, T. K. W. & Poon, L. L. M. Biology of influenza A virus. *Ann. N. Y. Acad. Sci.* 1102, 1–25 (2007).
9. Nakatsu, S. *et al.* Influenza C and D viruses package eight organized ribonucleoprotein complexes. *J. Virol.* 92, JVI.02084–17 (2018).
10. Brown, I. H., Harris, P. A. & Alexander, D. J. Serological studies of influenza viruses in pigs in Great Britain 1991–2. *Epidemiol. Infect.* 114, 511 (1995).
11. Osterhaus, A. D., Rimmelzwaan, G. F., Martina, B. E., Bestebroer, T. M. & Fouchier, R. A. Influenza B virus in seals. *Science* 288, 1051–3 (2000).
12. Webster, R. G., Bean, W. J., Gorman, O. T., Chambers, T. M. & Kawaoka, Y. Evolution and ecology of influenza A viruses. *Microbiol. Rev.* 56, 152–79 (1992).
13. Iuliano, A. D. *et al.* Estimates of global seasonal influenza-associated respiratory mortality: a modelling study. *Lancet* 391, 1285–1300 (2018).
14. te Velhuis, A. J. W. & Fodor, E. Influenza virus RNA polymerase: insights into the mechanisms of viral RNA synthesis. *Nat. Rev. Microbiol.* 14, 479–493 (2016).
15. Taubenberger, J. K. & Kash, J. C. Influenza virus evolution, host adaptation, and pandemic formation. *Cell Host Microbe* 7, 440–51 (2010).
16. Johnson, N. P. A. S. & Mueller, J. Updating the accounts: global mortality of the 1918–1920 Spanish influenza pandemic. *Bull. Hist. Med.* 76, 105–15 (2002).
17. Scholtissek, C. Molecular evolution of influenza viruses. *Virus Genes* 11, 209–15 (1995).

18. Nelson, M. I. & Holmes, E. C. The evolution of epidemic influenza. *Nat. Rev. Genet.* 8, 196–205 (2007).
19. Scheiffele, P., Rietveld, A., Wilk, T. & Simons, K. Influenza viruses select ordered lipid domains during budding from the plasma membrane. *J. Biol. Chem.* 274, 2038–44 (1999).
20. Dadonaite, B., Vijayakrishnan, S., Fodor, E., Bhella, D. & Hutchinson, E. C. Filamentous influenza viruses. *J. Gen. Virol.* 97, 1755–1764 (2016).
21. Chu, C. M., Dawson, I. M. & Elford, W. J. Filamentous forms associated with newly isolated influenza virus. *Lancet* 602–3 (1949).
22. Elford, W. J., Andrewes, C. H. & Tang, F. F. The sizes of the viruses of human and swine influenza as determined by ultrafiltration. *Br J Exp Pathol.* 17(1): 51–53 (1936).
23. Roberts, P. C., Lamb, R. A. & Compans, R. W. The M1 and M2 proteins of influenza A virus are important determinants in filamentous particle formation. *Virology* 240, 127–137 (1998).
24. Klemm, C., Boergeling, Y., Ludwig, S. & Ehrhardt, C. Immunomodulatory nonstructural proteins of influenza A viruses. *Trends in Microbiology* (2018).
25. Samji, T. Influenza A: understanding the viral life cycle. *Yale J. Biol. Med.* 82, 153–9 (2009).
26. Nayak, D. P., Hui, E. K.-W. & Barman, S. Assembly and budding of influenza virus. *Virus Res.* 106, 147–165 (2004).
27. Nayak, D. P., Balogun, R. A., Yamada, H., Zhou, Z. H. & Barman, S. Influenza virus morphogenesis and budding. *Virus Res.* 143, 147–61 (2009).
28. Morris, D. E., Cleary, D. W. & Clarke, S. C. Secondary bacterial infections associated with influenza pandemics. *Front. Microbiol.* 8, 1041 (2017).
29. Skehel, J. J. & Wiley, D. C. Receptor binding and membrane fusion in virus entry: the influenza hemagglutinin. *Annu. Rev. Biochem.* 69, 531–569 (2000).
30. Huang, Q. *et al.* Early steps of the conformational change of influenza virus hemagglutinin to a fusion active state: stability and energetics of the hemagglutinin. *Biochim. Biophys. Acta* 1614, 3–13 (2003).
31. Pinto, L. H., Holsinger, L. J. & Lamb, R. A. Influenza virus M2 protein has ion channel activity. *Cell* 69, 517–28 (1992).
32. Pinto, L. H. & Lamb, R. A. The M2 proton channels of influenza A and B viruses. *J. Biol. Chem.* 281, 8997–9000 (2006).

33. Görlich, D., Prehn, S., Laskey, R. A. & Hartmann, E. Isolation of a protein that is essential for the first step of nuclear protein import. *Cell* 79, 767–78 (1994).
34. te Velthuis, A. J. W. Common and unique features of viral RNA-dependent polymerases. *Cell. Mol. Life Sci.* 71, 4403–4420 (2014).
35. Fodor, E. The RNA polymerase of influenza A virus: mechanisms of viral transcription and replication. *Acta Virol.* 57, 113–22 (2013).
36. York, A. & Fodor, E. Biogenesis, assembly, and export of viral messenger ribonucleoproteins in the influenza A virus infected cell. *RNA Biol.* 10, 1274–1282 (2013).
37. Li, M.-L., Rao, P. & Krug, R. M. The active sites of the influenza cap-dependent endonuclease are on different polymerase subunits. *Embo J.* 20, 2078–2086 (2001).
38. Krug, R. M., Broni, B. A. & Bouloy, M. Are the 5' ends of influenza viral mRNAs synthesized *in vivo* donated by host mRNAs? *Cell* 18, 329–334 (1979).
39. Dhar, R., Chanock, R. M. & Lai, C. J. Nonviral oligonucleotides at the 5' terminus of cytoplasmic influenza viral mRNA deduced from cloned complete genomic sequences. *Cell* 21, 495–500 (1980).
40. Boulo, S., Akarsu, H., Ruigrok, R. W. H. & Baudin, F. Nuclear traffic of influenza virus proteins and ribonucleoprotein complexes. *Virus Res.* 124, 12–21 (2007).
41. Palese, P., Tobita, K., Ueda, M. & Compans, R. W. Characterization of temperature sensitive influenza virus mutants defective in neuraminidase. *Virology* 61, 397–410 (1974).
42. Conenello, G. M. & Palese, P. Influenza A Virus PB1-F2: A small protein with a big punch. *Cell Host Microbe* 2, 207–209 (2007).
43. Iverson, A. R. *et al.* Influenza virus primes mice for pneumonia from *Staphylococcus aureus*. *J. Infect. Dis.* 203, 880–888 (2011).
44. Kono, H. & Rock, K. L. How dying cells alert the immune system to danger. *Nature Reviews Immunology* 8, 279–289 (2008).
45. Ouyang, J. *et al.* NRAV, a long noncoding RNA, modulates antiviral responses through suppression of interferon-stimulated gene transcription. *Cell Host Microbe* 16, 616–626 (2014).
46. Yoneyama, M., Onomoto, K., Jogi, M., Akaboshi, T. & Fujita, T. Viral RNA detection by RIG-I-like receptors. *Curr. Opin. Immunol.* 32, 48–53 (2015).

47. Hiscott, J., Nguyen, T.-L. A., Arguello, M., Nakhaei, P. & Paz, S. Manipulation of the nuclear factor- $\kappa$ B pathway and the innate immune response by viruses. *Oncogene* 25, 6844–6867 (2006).
48. Kumar, H., Kawai, T. & Akira, S. Pathogen recognition by the innate immune system. *Int. Rev. Immunol.* 30, 16–34 (2011).
49. Alexopoulou, L., Holt, A. C., Medzhitov, R. & Flavell, R. A. Recognition of double-stranded RNA and activation of NF- $\kappa$ B by Toll-like receptor 3. *Nature* 413, 732–738 (2001).
50. Lund, J. M. *et al.* Recognition of single-stranded RNA viruses by Toll-like receptor 7. *Proc. Natl. Acad. Sci.* 101, 5598–5603 (2004).
51. Philpott, D. J., Sorbara, M. T., Robertson, S. J., Croitoru, K. & Girardin, S. E. NOD proteins: Regulators of inflammation in health and disease. *Nature Reviews Immunology* 14, 9–23 (2014).
52. Gross, O., Thomas, C. J., Guarda, G. & Tschopp, J. The inflammasome: An integrated view. *Immunol. Rev.* 243, 136–151 (2011).
53. Levy, D. E., Marié, I. J. & Durbin, J. E. Induction and function of type I and III interferon in response to viral infection. *Curr. Opin. Virol.* 1, 476–486 (2011).
54. Wang, J. *et al.* Differentiated human alveolar type II cells secrete antiviral IL-29 (IFN- 1) in response to influenza A infection. *J. Immunol.* 182, 1296–1304 (2009).
55. Ehrhardt, C. *et al.* Interplay between influenza A virus and the innate immune signaling. *Microbes and Infection* 12, 81–87 (2010).
56. García-Sastre, A. Induction and evasion of type I interferon responses by influenza viruses. *Virus Res.* 162, 12–18 (2011).
57. Chen, X. *et al.* Host immune response to influenza A virus infection. *Front. Immunol.* 9, 320 (2018).
58. Fernández, M. *et al.* *In vivo* and *in vitro* Induction of MxA Protein in Peripheral Blood Mononuclear Cells from Patients Chronically Infected with Hepatitis C Virus. *J. Infect. Dis.* 180, 262–267 (1999).
59. Yuan, W. & Krug, R. M. Influenza B virus NS1 protein inhibits conjugation of the interferon (IFN)-induced ubiquitin-like ISG15 protein. *EMBO J.* 20, 362–371 (2001).
60. Hale, B. G., Randall, R. E., Ortin, J. & Jackson, D. The multifunctional NS1 protein of influenza A viruses. *Journal of General Virology* 89, 2359–2376 (2008).
61. Melen, K. *et al.* Nuclear and nucleolar targeting of influenza A virus NS1 protein: striking differences between different virus subtypes. *J. Virol.* 81, 5995–6006 (2007).

62. Liedmann, S. *et al.* Viral suppressors of the RIG-I-mediated interferon response are pre-packaged in influenza virions. *Nat. Commun.* 5, 5645 (2014).
63. Ehrhardt, C. *et al.* Influenza A virus NS1 protein activates the PI3K/Akt pathway to mediate antiapoptotic signaling responses. *J. Virol.* 81, 3058–3067 (2007).
64. Kamal, R., Alymova, I. & York, I. Evolution and virulence of influenza A virus protein PB1-F2. *Int. J. Mol. Sci.* 19, 96 (2017).
65. West, A. P., Shadel, G. S. & Ghosh, S. Mitochondria in innate immune responses. *Nat. Rev. Immunol.* 11, 389–402 (2011).
66. Varga, Z. T. *et al.* The influenza virus protein PB1-F2 inhibits the induction of type I interferon at the level of the MAVS adaptor protein. *PLoS Pathog.* 7, (2011).
67. Yoshizumi, T. *et al.* Influenza A virus protein PB1-F2 translocates into mitochondria via Tom40 channels and impairs innate immunity. *Nat. Commun.* 5, 4713 (2014).
68. Reis, A. L. & McCauley, J. W. The influenza virus protein PB1-F2 interacts with IKK $\beta$  and modulates NF- $\kappa$ B signalling. *PLoS One* 8, (2013).
69. Pinar, A. *et al.* PB1-F2 peptide derived from avian influenza A virus H7N9 induces inflammation via activation of the NLRP3 inflammasome. *J. Biol. Chem.* 292, 826–836 (2017).
70. Lowy, F. D. *Staphylococcus aureus* infections. *N. Engl. J. Med.* 339, 520–532 (1998).
71. Kluytmans, J., van Belkum, A. & Verbrugh, H. Nasal carriage of *Staphylococcus aureus*: epidemiology, underlying mechanisms, and associated risks. *Clin. Microbiol. Rev.* 10, 505–20 (1997).
72. Tong, S. Y. C., Davis, J. S., Eichenberger, E., Holland, T. L. & Fowler, V. G. *Staphylococcus aureus* infections: epidemiology, pathophysiology, clinical manifestations, and management. (2015).
73. Cabot, R. C. *et al.* Case 6-1993-A 69-Year-Old Woman with a Sclerotic Lesion of the Femur and Pulmonary Nodules. *N. Engl. J. Med.* 328, 422–428 (1993).
74. Kipp, F. *et al.* Detection of *Staphylococcus aureus* by 16S rRNA directed in situ hybridisation in a patient with a brain abscess caused by small colony variants. *J. Clin. Pathol.* 56, 746–746 (2003).
75. Proctor, R. A., van Langevelde, P., Kristjansson, M., Maslow, J. N. & Arbeit, R. D. Persistent and relapsing infections associated with small-colony variants of *Staphylococcus aureus*. *Clin. Infect. Dis.* 20, 95–102 (1995).

76. Tabah, A. *et al.* Characteristics and determinants of outcome of hospital-acquired bloodstream infections in intensive care units: the EUROBACT International Cohort Study. *Intensive Care Med.* 38, 1930–1945 (2012).
77. Wertheim, H. F. L. *et al.* The role of nasal carriage in *Staphylococcus aureus* infections. *Lancet. Infect. Dis.* 5, 751–62 (2005).
78. Gordon, R. J. & Lowy, F. D. Pathogenesis of methicillin-resistant *Staphylococcus aureus* infection. *Clin. Infect. Dis.* 46, S350–S359 (2008).
79. Lina, G. *et al.* Involvement of Panton-Valentine Leukocidin-producing *Staphylococcus aureus* in primary skin infections and pneumonia. *Clin. Infect. Dis.* 29, 1128–1132 (1999).
80. Fuda, C. C. S., Fisher, J. F. & Mobashery, S.  $\beta$ -Lactam resistance in *Staphylococcus aureus*: the adaptive resistance of a plastic genome. *Cell. Mol. Life Sci.* 62, 2617–2633 (2005).
81. Tuchscher, L. *et al.* *Staphylococcus aureus* phenotype switching: an effective bacterial strategy to escape host immune response and establish a chronic infection. *EMBO Mol. Med.* 3, 129–41 (2011).
82. Tuchscher, L. *et al.* *Staphylococcus aureus* small-colony variants are adapted phenotypes for intracellular persistence. *J. Infect. Dis.* 202, 1031–1040 (2010).
83. Proctor, R. A. *et al.* Small colony variants: a pathogenic form of bacteria that facilitates persistent and recurrent infections. *Nat. Rev. Microbiol.* 4, 295–305 (2006).
84. Parker, D. & Prince, A. Immunopathogenesis of *Staphylococcus aureus* pulmonary infection. *Semin. Immunopathol.* 34, 281–297 (2012).
85. Gómez, M. I. *et al.* *Staphylococcus aureus* protein A induces airway epithelial inflammatory responses by activating TNFR1. *Nat. Med.* 10, 842–848 (2004).
86. Xing, Z. *et al.* Host immune and apoptotic responses to avian influenza virus H9N2 in human tracheobronchial epithelial cells. *Am. J. Respir. Cell Mol. Biol.* 44, 24–33 (2011).
87. Von Aulock, S. *et al.* Lipoteichoic acid from is a potent stimulus for neutrophil recruitment. *Immunobiology* 208, 413–422 (2003).
88. Hoogerwerf, J. J. *et al.* Lung inflammation induced by lipoteichoic acid or lipopolysaccharide in humans. *Am. J. Respir. Crit. Care Med.*
89. Zivkovic, A. *et al.* TLR 2 and CD14 mediate innate immunity and lung inflammation to staphylococcal Panton-Valentine Leukocidin *in vivo*. *J. Immunol.* 186, 1608–1617 (2011).

90. Gómez, M. I., O'Seaghdha, M., Magargee, M., Foster, T. J. & Prince, A. S. *Staphylococcus aureus* protein A activates TNFR1 signaling through conserved IgG binding domains. *J. Biol. Chem.* 281, 20190–20196 (2006).
91. Quinn, G. A. & Cole, A. M. Suppression of innate immunity by a nasal carriage strain of *Staphylococcus aureus* increases its colonization on nasal epithelium. *Immunology* 122, 80–89 (2007).
92. Saba, S., Soong, G., Greenberg, S. & Prince, A. Bacterial Stimulation of Epithelial G-CSF and GM-CSF Expression Promotes PMN Survival in CF Airways. *Am. J. Respir. Cell Mol. Biol.* 27, 561–567 (2002).
93. Martin, F. J., Parker, D., Harfenist, B. S., Soong, G. & Prince, A. Participation of CD11c<sup>+</sup> leukocytes in methicillin-resistant *Staphylococcus aureus* clearance from the lung. *Infect. Immun.* 79, 1898–1904 (2011).
94. Soong, G. *et al.* *Staphylococcus aureus* protein A mediates invasion across airway epithelial cells through activation of RhoA GTPase signaling and proteolytic activity. *J. Biol. Chem.* 286, 35891–35898 (2011).
95. Charrel-Dennis, M. *et al.* TLR-Independent type I interferon induction in response to an extracellular bacterial pathogen via intracellular recognition of its DNA. *Cell Host Microbe* 4, 543–554 (2008).
96. Martin, F. J. *et al.* *Staphylococcus aureus* activates type I IFN signaling in mice and humans through the Xr repeated sequences of protein A. *J. Clin. Invest.* 119, 1931–1939 (2009).
97. Bergsbaken, T., Fink, S. L. & Cookson, B. T. Pyroptosis: Host cell death and inflammation. *Nature Reviews Microbiology* 7, 99–109 (2009).
98. Munoz-Planillo, R., Franchi, L., Miller, L. S. & Nunez, G. A. Critical role for hemolysins and bacterial lipoproteins in *Staphylococcus aureus*-induced activation of the NLRP3 inflammasome. *J. Immunol.* 183, 3942–3948 (2009).
99. Lappalainen, U., Whitsett, J. A., Wert, S. E., Tichelaar, J. W. & Bry, K. Interleukin-1 $\beta$  causes pulmonary inflammation, emphysema, and airway remodeling in the adult murine lung. *Am. J. Respir. Cell Mol. Biol.* 32, 311–318 (2005).
100. Martinon, F., Burns, K. & Tschopp, J. The Inflammasome: A molecular platform triggering activation of inflammatory caspases and processing of proIL- $\beta$ . *Mol. Cell* 10, 417–426 (2002).
101. Shimada, T. *et al.* *Staphylococcus aureus* evades lysozyme-based peptidoglycan digestion that links phagocytosis, inflammasome activation, and IL-1 $\beta$  secretion. *Cell Host Microbe* 7, 38–49 (2010).

102. Bosch, A. A. T. M., Biesbroek, G., Trzcinski, K., Sanders, E. A. M. & Bogaert, D. Viral and bacterial interactions in the upper respiratory tract. *PLoS Pathogens* 9, e1003057 (2013).
103. McCullers, J. A. Insights into the interaction between influenza virus and pneumococcus. *Clinical Microbiology Reviews* 19, 571–582 (2006).
104. Morens, D. M., Taubenberger, J. K. & Fauci, A. S. Predominant role of bacterial pneumonia as a cause of death in pandemic influenza: implications for pandemic influenza preparedness. *J. Infect. Dis.* 198, 962–970 (2008).
105. Brundage, J. F. Interactions between influenza and bacterial respiratory pathogens: implications for pandemic preparedness. *Lancet Infect. Dis.* 6, 303–312 (2006).
106. Brundage, J. F. & Shanks, G. D. Deaths from bacterial pneumonia during 1918–19 Influenza pandemic. *Emerg. Infect. Dis.* 14, 1193–1199 (2008).
107. Bellinghausen, C. *et al.* Exposure to common respiratory bacteria alters the airway epithelial response to subsequent viral infection. *Respir. Res.* 17, 68 (2016).
108. McCullers, J. A. & Bartmess, K. C. Role of neuraminidase in lethal synergism between influenza virus and *Streptococcus pneumoniae*. *J. Infect. Dis.* 187, 1000–1009 (2005).
109. Peltola, V. T., Murti, K. G. & McCullers, J. A. Influenza virus neuraminidase contributes to secondary bacterial pneumonia. *J. Infect. Dis.* 192, 249–257 (2005).
110. McAuley, J. *et al.* Rapid evolution of the PB1-F2 virulence protein expressed by human seasonal H3N2 influenza viruses reduces inflammatory responses to infection. *Virology* 14, 162 (2017).
111. Vareille, M., Kieninger, E., Edwards, M. R. & Regamey, N. The airway epithelium: Soldier in the fight against respiratory viruses. *Clin. Microbiol. Rev.* 24, 210–229 (2011).
112. Kamada, N., Chen, G. Y., Inohara, N. & Núñez, G. Control of pathogens and pathobionts by the gut microbiota. *Nature Immunology* 14, 685–690 (2013).
113. Hooper, L. V., Littman, D. R. & Macpherson, A. J. Interactions between the microbiota and the immune system. *Science* 336, 1268–1273 (2012).
114. Chervonsky, A. V. Influence of microbial environment on autoimmunity. *Nat. Immunol.* 11, 28–35 (2010).

115. Wang, B., Yao, M., Lv, L., Ling, Z. & Li, L. The Human Microbiota in Health and Disease. *Engineering* 3, 71–82 (2017).
116. Chen, K., Shanmugam, N. K. N., Pazos, M. A., Hurley, B. P. & Cherayil, B. J. Commensal bacteria-induced inflammasome activation in mouse and human macrophages is dependent on potassium efflux but does not require phagocytosis or bacterial viability. *PLoS One* 11, e0160937 (2016).
117. Ichinohe, T. *et al.* Microbiota regulates immune defense against respiratory tract influenza A virus infection. *Proc. Natl. Acad. Sci.* 108, 5354–5359 (2011).
118. Cabello, H. *et al.* Bacterial colonization of distal airways in healthy subjects and chronic lung disease: A bronchoscopic study. *Eur. Respir. J.* 10, 1137–1144 (1997).
119. Zalacain, R. *et al.* Predisposing factors to bacterial colonization in chronic obstructive pulmonary disease. *Eur. Respir. J.* 13, 343–348 (1999).
120. Monsó, E. *et al.* Risk factors for lower airway bacterial colonization in chronic bronchitis. *Eur. Respir. J.* 13, 338–42 (1999).
121. Gulraiz, F., Bellinghausen, C., Bruggeman, C. A. & Stassen, F. R. Haemophilus influenzae increases the susceptibility and inflammatory response of airway epithelial cells to viral infections. *FASEB J.* 29, 849–858 (2015).
122. Heinrich, A. *et al.* Moraxella catarrhalis decreases antiviral innate immune responses by down-regulation of TLR3 via inhibition of p53 in human bronchial epithelial cells. *FASEB J.* 30, 2426–2434 (2016).
123. Sajjan, U. S. *et al.* H. influenzae potentiates airway epithelial cell responses to rhinovirus by increasing ICAM-1 and TLR3 expression. *FASEB J.* 20, 2121–2123 (2006).
124. Livak, K. J. & Schmittgen, T. D. Analysis of relative gene expression data using Real-Time Quantitative PCR and the 2- $\Delta\Delta$ CT Method. *Methods* 25, 402–408 (2001).
125. Bradford, M. M. A rapid and sensitive method for the quantitation of microgram quantities of protein utilizing the principle of protein-dye binding. *Anal. Biochem.* 72, 248–54 (1976).
126. Probst, H. C., Lagnel, J., Kollias, G. & van den Broek, M. Inducible transgenic mice reveal resting dendritic cells as potent inducers of CD8<sup>+</sup> T cell tolerance. *Immunity* 18, 713–20 (2003).

127. Chertow, D. S. & Memoli, M. J. Bacterial co-infection in influenza: A grand rounds review. *JAMA - J. Am. Med. Assoc.* 309, 275–282 (2013).
128. Löffler, B. *et al.* Pathogenesis of *Staphylococcus aureus* necrotizing pneumonia: The role of PVL and an influenza co-infection. *Expert Review of Anti-Infective Therapy* 11, 1041–1051 (2013).
129. Taubenberger, J. K. & Morens, D. M. 1918 Influenza: The mother of. *Emerg. Infect. Dis.* 12, 15–22 (2006).
130. Perales, B. *et al.* The replication activity of influenza virus polymerase is linked to the capacity of the PA subunit to induce proteolysis. *J. Virol.* 74, 1307–12 (2000).
131. Mori, I. *et al.* *In vivo* induction of apoptosis by influenza virus. *J. Gen. Virol.* 76, 2869–2873 (1995).
132. Hinshaw, V. S., Olsen, C. W., Dybdahl-Sissoko, N. & Evans, D. Apoptosis: a mechanism of cell killing by influenza A and B viruses. *J. Virol.* 68, 3667–73 (1994).
133. McCullers, J. A. Effect of antiviral treatment on the outcome of secondary bacterial pneumonia after influenza. *J. Infect. Dis.* 190, 519–526 (2004).
134. Siegel, S. J., Roche, A. M. & Weiser, J. N. Influenza promotes pneumococcal growth during coinfection by providing host sialylated substrates as a nutrient source. *Cell Host Microbe* 16, 55–67 (2014).
135. Tashiro, M., Ciborowski, P., Klenk, H.-D., Pulverer, G. & Rott, R. Role of *Staphylococcus* protease in the development of influenza pneumonia. *Nature* 325, 536–537 (1987).
136. Tashiro, M. *et al.* Synergistic role of staphylococcal proteases in the induction of influenza virus pathogenicity. *Virology* 157, 421–430 (1987).
137. McGilligan, V. E. *et al.* *Staphylococcus aureus* Activates the NLRP3 Inflammasome in Human and Rat Conjunctival Goblet Cells. *PLoS One* 8, e74010 (2013).
138. Melehani, J. H. & Duncan, J. A. Inflammasome activation can mediate tissue-specific pathogenesis or protection in *Staphylococcus aureus* infection. *Curr. Top. Microbiol. Immunol.* 397, 257–82 (2016).
139. Parker, D. & Prince, A. Type I interferon response to extracellular bacteria in the airway epithelium. *Trends in Immunology* 32, 582–588 (2011).
140. Warnking, K. *et al.* Super-infection with *Staphylococcus aureus* inhibits influenza virus-induced type I IFN signalling through impaired STAT1-STAT2 dimerization. *Cell. Microbiol.* 17, 303–317 (2015).

141. Horimoto, T. & Kawaoka, Y. Influenza: Lessons from past pandemics, warnings from current incidents. *Nature Reviews Microbiology* 3, 591–600 (2005).